

---

**This manuscript is an EarthArXiv preprint**, and has been submitted for publication in **Palaeogeography, Palaeoclimatology, Palaeoecology**. Please note that the manuscript has yet to be formally accepted for publication. Subsequent versions of this manuscript may have slightly different content. If accepted, the final version of this manuscript will be available via the 'Peer-reviewed Publication DOI' link on the right-hand side of this webpage. Please feel free to contact any of the authors; we welcome feedback.

---

1 **Architecture and controls of thick, intensely bioturbated, storm-influenced shallow-**  
2 **marine successions: an example from the Jurassic Neuquén Basin (Argentina)**

3

4 Schwarz, E.<sup>1\*</sup>, Poyatos-Moré, M.<sup>2</sup>, Boya, S.<sup>3</sup>, Gomis-Cartesio, L.<sup>4</sup> and Midtkandal, I.<sup>2</sup>

5 1- Centro de Investigaciones Geológicas, Universidad Nacional de La Plata-CONICET, Argentina

6 2- Department of Geosciences, University of Oslo, Norway

7 3- Departament de Geologia, Universitat Autònoma de Barcelona, Spain

8 4- Equinor ASA, Research Centre, Bergen, Norway

9

10 \*Schwarz, E. Corresponding author. Email: [eschwarz@cig.museo.unlp.edu.ar](mailto:eschwarz@cig.museo.unlp.edu.ar)

11 Poyatos-Moré, M. Email: [miquel.poyatos-more@geo.uio.no](mailto:miquel.poyatos-more@geo.uio.no)

12 Boya, S.: [salvaboya@gmail.com](mailto:salvaboya@gmail.com)

13 Gomis-Cartesio, L.: [LUZG@equinor.com](mailto:LUZG@equinor.com)

14 Midtkandal, I.: [ivar.midtkandal@geo.uio.no](mailto:ivar.midtkandal@geo.uio.no)

15

16 This version: Words: about 5800; 11 Figures, 2 Tables.

17 Running title: Architecture and controls of thick, intensely bioturbated, storm-influenced  
18 successions

19

20 **ABSTRACT**

21 Thick (>100 m-thick), highly bioturbated storm-influenced shallow-marine deposits are not  
22 frequent in the stratigraphic record, but they tend to be unusually common in aggradational to  
23 retrogradational successions. Individual storm-event beds have typically low preservation in these  
24 successions, yet depositional settings are characterized on the basis of storms processes. We  
25 present a sedimentological study of a thick, bioturbated exhumed succession deposited during the  
26 early post-rift stage of the Neuquén Basin (Argentina) and compare its stratigraphic record with  
27 examples developed worldwide, in order to discuss controlling factors on the total destruction of  
28 storm-event beds during several million years.

29 The Bardas Blancas Formation (170-220 m thick) is dominated by muddy sandstones and  
30 sandy mudstones, but it also includes subordinate proportions of clean sandstones and pure  
31 mudstones, collectively representing different environments of a storm-influenced shoreface-  
32 offshore system. The offshore transition and proximal offshore strata invariably comprises intensely  
33 bioturbated deposits, with only a few preserved HCS-sandstone beds. The unit shows a long-term  
34 aggradational pattern involving ca. 7-10 Myr and is associated with low riverine influence.

35 By combining the observations and interpretations of the Bardas Blancas Formation with  
36 other subsurface and exhumed intensely bioturbated, shallow-marine successions we dispute the  
37 general assumption that they can be associated to low frequency or low magnitude of storms.  
38 Alternatively, we propose that the long-lived efficiency of benthic fauna on destroying most if not  
39 all the storm-event beds that reached the offshore-transition sector, results from the combination  
40 of two or three factors: deposition in relatively confined marine depocentres, persistent low riverine  
41 influence, and long-term aggradational stacking pattern. As these conditions can be recreated in a  
42 variety of basin styles, such as rift, early post-rift, and foreland settings, the recognition of thick,  
43 bioturbated successions as the ones discussed here can be used to infer more realistic constrains  
44 for depositional models and better predict facies distribution in these storm-influenced systems.

45

46 Key words: storm events, biogenic destruction, shallow-marine strata, Jurassic, Bardas Blancas  
47 Formation, Neuquén Basin.

48

49

## 50 **1. INTRODUCTION**

51         The deposition and preservation of individual storm-related event beds in shallow-marine  
52 settings have been reported and extensively discussed in the literature (Niedoroda et al., 1989;  
53 Wheatcroft, 1990; Snedden and Nummedal, 1991; MacEachern and Pemberton 1992; among many  
54 others). MacEachern and Pemberton (1992) characterized three types of shorefaces based on the  
55 intensity and frequency of storms: intense, moderate, and weak (low-energy) shorefaces. It is  
56 typically assumed that a thoroughly bioturbated succession with little or no preserved storm-event  
57 beds within a storm-influenced shoreface-offshore system would represent weakly storm-affected  
58 shorefaces dominated by fair-weather deposits (MacEachern and Pemberton 1992; MacEachern et  
59 al., 1999, Pemberton et al., 2012).

60         Thick successions (>100 m-thick) of storm-influenced, shallow-marine deposits characterized  
61 by highly bioturbated strata are not frequent in the stratigraphic record. However, they tend to be  
62 unusually common in rift to early post-rift stages of the Central Graben (Fraser et al., 2003; Gowland,  
63 1996; Howell et al., 1996; Baniak et al., 2014), in rift stages of the Viking Graben (Råvnas et al., 1997;  
64 Løseth et al., 2009), and in early post-rift stages of the Neuquén Basin (Veiga et al., 2013). Other  
65 unusual examples of highly bioturbated, storm-influenced successions include the Bridport Sand  
66 Formation in the extensional Wessex Basin (Morris et al., 2006) and the Late Cretaceous Emery  
67 Sandstone Member of the Mancos Shale in the Western Interior foreland basin (Edwards et al.,  
68 2005). However, a thorough analysis of all these examples to test if they can be simply placed in the  
69 low-energy shoreface end-member of the MacEachern and Pemberton (1992) spectrum, or if there  
70 are other controlling factors that contribute to produce thick bioturbated storm-influenced  
71 successions, has not yet been attempted.

72         In this study, we present a detailed sedimentological study of a thick, highly bioturbated  
73 succession exposed in the northern Neuquén Basin (Lower-Middle Jurassic, Bardas Blancas  
74 Formation) with the following objectives: a) to describe and analyse an intensively bioturbated,  
75 storm-influenced shallow-marine succession, b) to compare the stratigraphic record of the Bardas  
76 Blancas Formation with thick, intensively bioturbated units from other basins, c) discuss combination  
77 of several depositional controls that contribute to the complete destruction of original sedimentary  
78 structures and storm-event beds during several million years.

## 80 2. GEOLOGIC AND STRATIGRAPHIC SETTING

81 The Neuquén Basin is located on the eastern side of the Andes in west-central Argentina,  
82 between latitudes 32° and 40° South, covering an area of over 150,000 km<sup>2</sup> (Fig. 1). It comprises a  
83 nearly continuous record of up to 6,000 m of stratigraphy from the Late Triassic to the Early Cenozoic  
84 and is one of the most important petroleum provinces of the country (e.g. Uliana and Legarreta,  
85 1993). The sedimentary record of the Neuquén Basin includes continental and marine siliciclastics,  
86 carbonates, and evaporites, deposited under a variety of basin styles (Legarreta and Uliana, 1991;  
87 Howell et al., 2005).

88 During the Late Triassic to Early Jurassic, the western border of Gondwana was characterized  
89 by large transcurrent fault systems. This led to extensional tectonics within the Neuquén Basin and  
90 the formation of a series of narrow, relatively isolated depocentres (Franzese and Spalletti, 2001),  
91 which were filled mostly with volcanic and continental successions (Franzese et al., 2006; D'Elía et  
92 al., 2015). Due to continuous subduction at the proto-Pacific margin of Gondwana, a transition from  
93 syn- to post-rift conditions occurred in the late Early Jurassic (Vergani et al. 1995), marked by the  
94 first marine incursion in the basin (Gulisano et al., 1981; Veiga et al., 2013). The Neuquén Basin  
95 became a back-arc depocentre characterized by regional, slow subsidence (sag/post-rift phase) that  
96 lasted to the end of the Early Cretaceous (Legarreta and Uliana, 1991). In the earliest stage of the  
97 post-rift phase, sediment gravity flows and mass movements were particularly common in marine  
98 settings, and this has been related to steep gradients (e.g., Legarreta and Uliana, 1996; Burgess et  
99 al., 2000; Privat et al., 2020). In this context, low-amplitude eustatic fluctuations, as well as short-  
100 lived events of tectonic inversion, probably had a strong influence during the entire post-rift  
101 evolution (Legarreta and Uliana, 1991; Howell et al., 2005), but inherited topography and  
102 differential compaction had been invoked as potential local factors in the development of early post-  
103 rift strata in different sectors of the basin (Burgess et al. 2000; Cristallini et al., 2009; Veiga et al.,  
104 2013; Privat et al., 2020).

105 The Cuyo Group represents the early post-rift sedimentation all across the Neuquén Basin  
106 (Figs. 1, 2). It commonly overlies the Precuyano volcanic and volcanoclastic succession deposited  
107 during the syn-rift stage (Gulisano et al. 1984), but it can also rest directly upon Paleozoic volcanic  
108 or plutonic rocks (e.g., Choyoi Group, Fig. 2). The Cuyo Group spans from Early to Middle Jurassic  
109 and comprises deep-marine to continental deposits in different proportion depending on the

110 position in the basin, with a general east (proximal)-distal (west) depositional trend (Gulisano et al.  
111 1984; Arregui et al., 2011). In the west-central sector of the Neuquén Basin (Fig. 1), the succession  
112 represents continuing deep-water sedimentation, strongly influenced by sediment gravity flows and  
113 mass-transport processes (Burgess et al. 2000, Hodgson et al., 2018), and is collectively known as  
114 the Los Molles Formation (Gulisano and Gutiérrez Pleimling, 1994). In the study area, in the east-  
115 central sector of the basin (Fig. 2), early post-rift sediments deposited mostly in shallow-marine  
116 settings (Veiga et al., 2013), and accumulation started in the Late Toarcian–Aalenian (Riccardi 2008;  
117 Spalletti et al. 2012). Lithographically, in this region the Cuyo Group includes the Bardas Blancas, Los  
118 Molles and Lajas formations (Gulisano and Gutiérrez Pleimling 1994; Spalletti et al. 2012; Veiga et  
119 al., 2013) (Fig. 2). The Bardas Blancas Formation is the focus of this contribution.

120

### 121 **3. STUDY AREA AND PREVIOUS WORK**

122 Veiga et al. (2013) provided a detailed architectural and sequence stratigraphic analysis of the  
123 Bardas Blancas Formation in the study area, integrating outcrop and subsurface information from a  
124 3,000 km<sup>2</sup> area. They included two outcrop sections in the western and eastern sectors of the Sierra  
125 de Reyes anticline and several wells in the eastern subsurface region (Fig. 2). This study provides a  
126 framework in which to place the detailed sedimentological and ichnological analysis of the western  
127 outcrops of the Bardas Blancas Formation in the Sierra de Reyes anticline (Fig. 3A).

128 The Sierra de Reyes anticline is located in the southernmost sector of the Malargüe fold and  
129 thrust belt, which is the product of tectonic inversion during Late Cretaceous-Neogene time  
130 (Giambiagi et al., 2009). The inversion in this region is related to reactivation of Mesozoic normal  
131 faults and new reverse structures that transferred shortening to the east (Giambiagi et al., 2009;  
132 Sagripanti et al., 2014). The study area in the western flank of the Sierra de Reyes anticline is about  
133 5 by 1.5 km, and strata is mostly dipping 30-20 degrees to the east. The Bardas Blancas Formation  
134 is exposed through a series of west-east gullies in which the main sedimentary sections were  
135 measured (Fig. 3B). A few reverse faults affect the stratigraphy but for the most part the outcrop is  
136 laterally continuous and allows reconstruction by means of key stratigraphic markers.

137 The Bardas Blancas Formation (170-220 m thick) is dominated by muddy sandstones and  
138 sandy mudstones, but it also includes subordinate proportions of coarser deposits (up to pebbly  
139 sandstones) and pure mudstones. The unit unconformably overlies the syn-rift volcanoclastic

140 deposits of the Remoredo Formation all across the area (Figs. 3B, 4A), but the tops shows different  
141 vertical relationships. In the southern sector of the study area (and in the Quebrada de la Estrechura  
142 section, Figs. 2, 3A), the Bardas Blancas Formation rapidly grades into a pure mudstone, organic-rich  
143 unit defined as Los Molles Formation (Gulisano and Gutiérrez Pleimling, 1994; Spalletti et al., 2012)  
144 (Fig. 4B, C). The thickness of the Los Molles reaches 20 m in the Agua del Ñaco section, and it thins  
145 and pinches out to the north. In the Agua del Campo section, the Bardas Blancas strata are sharply  
146 overlying by bioclastic and pebbly sandstones of the La Estrechura Member of the Lotena Formation  
147 (Veiga et al., 2011; Veiga et al., 2013). Biostratigraphic data based on ammonites of the study  
148 succession indicates that the Bardas Blancas Formation in the study area spans from the Late  
149 Toarcian to the Early Bathonian (Spalletti et al. 2012) (Fig. 2). According to present numerical ages  
150 this time span would represent no less than 7 Myr and as much as 10 Myr. Further to the west of  
151 the study area, time-equivalent deposits of the Bardas Blancas Formation would be dominantly  
152 composed of mudstone strata of the Los Molles Formation, but they occur mostly in subsurface  
153 (e.g., well BjDC.x-1 in Fig. 2).

154 The sedimentology and stratigraphy of the Bardas Blancas Formation and its transition to Los  
155 Molles Formation in the study area was recorded by detailed logging of two main sections (Agua de  
156 Heredia and Agua del Ñaco sections, Figs. 3B, 4) and complemented with information extracted  
157 from the Agua del Campo section of Veiga et al. (2013). Sedimentological data were recorded in  
158 each section (texture, sedimentary structures, palaeocurrents), along with ichnofaunal,  
159 macrofaunal and taphonomic information. Bioturbation intensity was characterized using the  
160 Bioturbation Index (BI 0-6) defined by Taylor & Goldring (1993). Sand-silt-mud content in  
161 bioturbated facies was visually estimated by X10 lenses.

162

#### 163 **4. FACIES ASSOCIATIONS AND DEPOSITIONAL MODEL**

164 The facies and facies associations of the Bardas Blancas Formation and its transition to Los  
165 Molles Formation are presented in Table 1. Six facies associations have been defined for the study  
166 interval including: FA1 - Delta front, FA2 - Upper shoreface, FA3 - Lower shoreface, FA4 - Offshore  
167 transition, FA5 - Proximal offshore, and FA6 - Distal offshore. The definition and interpretation of  
168 these facies associations is broadly in agreement with the proposed by Veiga et al. (2013), except  
169 for FA1 and FA2 that are presented differently. Hereby we present a short description of facies  
170 associations and their interpretation and subsequently describe the inferred depositional model.

171

#### 172 **4.1. Delta front (FA1)**

173 Facies association FA1 occurs only at the base of the unit and only locally along the strike of  
174 the study area. This FA is dominated by conglomerates with quartz and volcanic pebbles (up to 5  
175 cm-long), mudstone rip-up clasts and bioclasts in a chaotic to organized fabric, interbedded with  
176 pebbly sandstones with planar cross-stratification or horizontal lamination (Table 1, Fig. 5A). This  
177 association is interpreted to represent a high-energy nearshore setting, heavily influenced by coarse  
178 terrestrial input of river-related hyperpycnal flows, and partly reworked by subordinate coastal  
179 processes (Veiga et al., 2013).

180

#### 181 **4.2. Upper shoreface (FA2)**

182 Facies association FA2 is composed of amalgamated fine- to medium-grained sandstones  
183 mostly with trough cross-stratification and occasional lenses of highly fragmented bioclasts (Fig. 5B).  
184 Bioturbation is absent to low with sparse *Ophiomorpha* (Table 1). This association is thought to  
185 reflect a wave-dominated, upper-shoreface setting, intensely affected by longshore currents  
186 (Walker and Plint, 1982; Isla et al., 2020).

187

#### 188 **4.3. Lower shoreface (FA3)**

189 Facies association FA3 mostly comprises tabular very fine- to fine-grained sandstones with  
190 HCS, and subordinated SCS, plane bed, and symmetrical ripples (Fig. 5C). Bioturbation intensity  
191 ranges significantly (BI 2-5) and is dominated by *Skolithos* ichnofacies (Table 1). This association is  
192 interpreted as a lower-shoreface setting dominated by deposits related to storm-surge, purely  
193 oscillatory or combined flows (Walker and Plint, 1992, Dumas and Arnott, 2006) with high re-  
194 mobilization potential, and associated low preservation of fair-weather sediments.

195

#### 196 **4.4. Offshore transition (FA4)**

197 Facies association FA4 is mostly composed of tabular and massive muddy sandstones and  
198 subordinated sandy mudstones (Fig. 5D). Bioturbation is mostly high (BI 5-6), locally moderate (BI



199 4), and is dominated by a highly diverse *Cruziana* ichnofacies (Table 1) in which *Teichichnus* and  
200 *Chondrites* are dominant (Fig. 6A, B). Infrequently, medium- to thin-bedded, very-fine grained  
201 sandstones with HCS are recorded in this association. These beds invariably show an increment of  
202 bioturbation at the top, passing abruptly to bioturbated muddy sandstones. This association  
203 represents an offshore-transition setting, immediately below the fair-weather wave base (Reading  
204 & Collinson, 1996). Storm-derived flows delivered sand to distal marine settings, but post-  
205 depositional bioturbation homogenized muds and sandy event beds into muddy sandstones in  
206 almost all cases.

207

#### 208 **4.5. Proximal offshore (FA5)**

209 Facies association FA5 is dominated by massive sandy and silty mudstones forming tabular  
210 beds with diffuse bedding planes (Fig. 5E). Bioturbation is systematically high (BI 5-6) and  
211 represented by a distal expression of the *Cruziana* ichnofacies (Table 1). Burrows of *Chondrites*,  
212 *Rhizocorallium*, and *Zoophycos* are sporadic in outcrops (Fig. 6C, D), whereas smaller traces such as  
213 *Phycosiphon* or *Helminthopsis* are commonly observed in cores of these sandy and silty mudstones  
214 (Veiga et al., 2013, their figure 9c). As in FA4, very uncommon discrete sandstone beds occur  
215 interbedded in this association, but they are finer grained and thinner (Table 1). Due to the relatively  
216 lower proportion of sand material in this association than in FA4, FA5 is interpreted to represent a  
217 proximal-offshore setting, i.e. the distal end of the running-distance of most storm-derived flows  
218 (Veiga et al., 2013).

219

#### 220 **4.6. Distal offshore (FA6)**

221 Facies association FA6 includes mudstone-dominated successions that are common at the  
222 base and top of the study interval (Fig. 2, 5F). At the base they consist of grey, massive mudstones  
223 with moderate bioturbation, represented by a *Zoophycos* ichnofacies commonly in cores (Veiga et  
224 al., 2013, their figure 9D). Medium- to thin-bedded conglomerates with extraformational pebbles  
225 and mudstone rip-up clasts are commonly interbedded in these massive mudstones. At the top of  
226 the unit FA6 is mostly represented by black, fissile (platy), unbioturbated shales, in which cm-thick  
227 tuffaceous layers occur. This section represents the transition to the Los Molles Formation. FA6 is  
228 interpreted to reflect the distalmost conditions of the marine system, i.e., a distal offshore to shelf,

229 but under two different conditions. Firstly, oxic sea-bottom conditions as well as sediment gravity  
230 flows depositing coarse material were common in the distal offshore of the early Bardas Blancas  
231 Formation. Conversely, inferred high organic contents and original lamination in the Los Molles  
232 Formation mudstones at the top of the study interval probably suggest long-lived dysoxic to anoxic  
233 conditions, in a saturated water–sediment interface (Doyle et al. 2005, Veiga et al., 2013).

234

#### 235 **4.7. Depositional model**

236 Except for FA1 that is solely recorded at the base of the Bardas Blancas Formation (Table 1),  
237 the remaining facies associations are commonly registered forming shallowing-upward successions  
238 that are up to a few 10s of m thick (Fig. 7). Thus, a well-defined storm- and wave-dominated  
239 shoreface-offshore depositional system is reconstructed for the unit. The upper-shoreface was  
240 dominated by migrating dunes and bars associated with long-shore currents (FA2), whereas the  
241 adjacent lower-shoreface setting mostly preserved event beds with hummocks sculpted by the  
242 development of storm-surge combined flows (FA3, Fig. 7). The shoreface bioturbation intensity and  
243 its distribution along dip follows normal patterns for wave-dominated shoreface-offshore systems,  
244 increasing downdip (Walker and Plint, 1992; Gowland, 1996; Hampson, 2000; MacEachern et al.  
245 2007; Schwarz et al., 2018).

246 In marked contrast, the preservation motifs and inferred conditions in the offshore transition  
247 (FA4) and proximal offshore (FA5) seems to be quite peculiar. These two adjacent settings record  
248 depositional conditions between the fair-weather wave base and storm wave base (Fig. 7), and  
249 reflect a gradual increment in the proportion of mud versus sand fraction in the resulting sediments,  
250 likely associated with the decreasing inability of storm-surge flows to export sand to more distal  
251 areas (Aigner et al., 1982). But as post-depositional homogenization of muds and sands is  
252 concerned, these two environments behave very similarly, providing a similar capacity of deposit-  
253 feeder organisms to rework almost 100% of the sands during inter-event periods. The fact that this  
254 condition prevailed for several million years (7-10 Myr) is not a commonly reported motif for  
255 examples worldwide and is further discussed in this contribution.

256 As for the distalmost segment of the shoreface-offshore system for most Bardas Blancas  
257 Formation, accumulation of muds is considered to have been dominantly from settling out of  
258 suspensions in very low-energy hydrodynamic settings (FA6). Debris flows transporting gravel were

259 common in early stages of the system (Fig. 7), but probably became infrequent later in its evolution,  
260 allowing to produce a mud-rich, distal offshore, occasionally colonized by *Zoophycos*-producing  
261 organisms. Distal offshore settings prevailed further to the west of the study area were substrate  
262 conditions probably remained constant during most of the Bardas Blancas deposition (Figs. 2, 7).  
263 But when a distal offshore setting was installed in the southern sector of the study area (Los Molles  
264 Formation), a shift to prevailing dysoxic-anoxic conditions appear to have dominated in a soupy  
265 substrate.

266

## 267 **5. ARCHITECTURE OF AN INTENSELY BIOTURBATED SUCCESSION**

268 The most distinctive feature of the Bardas Blancas Formation is that most of the proximal  
269 offshore (FA5) and offshore transition (FA4) strata comprises intensely bioturbated deposits (BI 5-  
270 6). Complete bioturbation (BI 6) is dominant, providing a complete structureless appearance of the  
271 beds in outcrop (Fig. 8A), due to total biogenic homogenization of the original deposits (Taylor and  
272 Goldring, 1993). It also typically prevents the identification of individual trace fossils. In these two  
273 facies associations, beds are defined by subtle variation in the sand-silt-mud content, usually aided  
274 by the weathering profile, where the muddier facies is less resistant (Fig. 8A). The relative  
275 dominance of muddy sandstones versus sandy and silty mudstones in a given interval places it in  
276 FA4 or FA5 (Fig. 8A, B). Individual beds range from 0.15 m up to 1.5 m and they almost invariably  
277 show planar, horizontal lower and upper contacts defining tabular beds at different scales, from a  
278 few 10s to 100s of meters in length (Fig. 8B, C).

279 The preserved volume of un-modified storm-generated deposits in these two facies  
280 associations is small, but still provides a window for interpreting the primary depositional processes  
281 and products. Where observed, these sandstone beds commonly have hummocky cross-  
282 stratification and are laterally continuous for up to a few 10s of meters (Fig. 9A, D). They have sharp,  
283 irregular bases overlying silty mudstones and invariably show irregular (indented), transitional to  
284 sharp tops into muddy sandstones (Fig. 9B, E). In these overlying muddy sandstones, bioturbation  
285 intensity is moderate to high (BI 4-5), and an ichnofabric dominated by *Chondrites* can be  
286 recognized in outcrop (Fig. 9C), but a more diverse assemblage including *Phycosiphon*, and  
287 *Zoophycos* has also been recorded in cores of the unit (Veiga et al., 2013). The overlying muddy  
288 sandstone becomes the “full bed” laterally from where the discrete storm-generated deposit is  
289 recognized (Fig. 9A, D).

290 The vertical distribution of facies associations in the study area allows to recognize  
291 shallowing-upward, 10s of meters-thick genetic units in the study interval of the Bardas Blancas  
292 Formation, identified as parasequences (Fig. 2). Shell beds mark flooding surfaces in places, and  
293 internally these parasequences are composed of bedsets with subtle stratigraphic boundaries (Fig.  
294 8D). Parasequences in the lower interval of the unit show a complete transition from mudstones of  
295 FA6 (distal offshore) to clean, trough cross-bedded sandstones of FA2 (upper shoreface)(Fig. 4),  
296 whereas in the middle and upper segments of the study interval, they are mostly composed of sandy  
297 mudstones and muddy sandstones of FA5 and FA4 (proximal offshore and offshore transition),  
298 sometimes with the presence of lower-shoreface HCS-sandstones at their top (FA4) (Figs. 8D, 9).  
299 Bioturbation intensity in the lower-shoreface deposits is either similar or lower than the one  
300 recorded in the underlying offshore-transition facies (Fig. 8D).

301 The vertical staking pattern and sequence architecture of the Bardas Blancas Formation in the  
302 study area was investigated by Veiga et al. (2013). Integrating outcrop and subsurface data they  
303 identified three parasequence sets within the study interval (Figs. 2, 4), individually representing  
304 alternating conditions from retrogradational (PS Sets I and III) to aggradational (PS Set II, Fig. 2)  
305 stacking patterns. Collectively these three units were interpreted as representing a long-term  
306 transgressive event (about 7-10 Myr) during the early post-rift stage of the basin, where sustained  
307 accommodation was probably provided by a combination of thermal subsidence, differential  
308 compaction of syn-rift deposits and eustatic rise (Veiga et al., 2013). The observed changes in the  
309 stacking patterns were attributed to the effect of inherited topography from the underfilled syn-rift  
310 hemigrabens, as sedimentation areas were expanding during progressive flooding and sediments  
311 were depositing in partially filled hemigraben-segments with different gradients.

312 The aggradational to retrogradational stacking pattern of Parasequence Sets II and III has a  
313 major impact in the resulting distinctive nature of the study succession. As a result of these  
314 particular conditions, about 100 m of the Bardas Blancas Formation in the study area are dominated  
315 by a vertical stacking of almost completely homogenized deposits of FA4 and FA5 (Figs. 4, 8 and 9).  
316 The resulting stratigraphy is a storm-generated, but highly bioturbated, thick monotonous  
317 succession, with very little grain size variation (muddy sandstones to sandy mudstones), virtual  
318 absence of preserved primary physical (depositional) structures, bedding contacts that are  
319 invariably horizontal, and scattered fossil remains that rarely produce distinct shell concentrations.

320 The potential combination of factors allowing for such exceptional resultant stratigraphy is  
321 discussed below.

322

## 323 **6. DISCUSSION**

### 324 **6.1. Thick bioturbated storm-influenced shallow-marine successions: where?**

325 The preservation potential of individual storm-related event beds (or tempestites) in shallow-  
326 marine settings and the lam-scam textures resulting from partial to total destruction of these event  
327 beds have been extensively reported and discussed (Wheatcroft, 1990; MacEachern and Pemberton  
328 1992; among many others). MacEachern and Pemberton (1992) characterized three types of  
329 shorefaces based on the intensity and frequency of storms: intense, moderate, and weak (low-  
330 energy). It is typically assumed that a thoroughly bioturbated succession with little or no preserved  
331 tempestites within a storm-influenced shoreface-offshore system would represent weakly storm-  
332 affected shorefaces dominated by fair-weather deposits. On the contrary, shorefaces with stacked,  
333 well-preserved tempestites would be interpreted as storm-dominated shorefaces (MacEachern and  
334 Pemberton 1992; MacEachern et al., 1999, Pemberton et al., 2012).

335 The Bardas Blancas Formation deposits interpreted to represent offshore-transition (partially  
336 equivalent of the “distal lower shoreface” of MacEachern et al. (1999) and proximal offshore  
337 settings are invariably composed of highly bioturbated muddy sandstones and sandy mudstones,  
338 and very few preserved tempestites. We demonstrate that all the preserved deposits in those  
339 settings are in fact the total biogenic homogenization of sediments (sand, silt, and mud) laid down  
340 by storm-surge flows. If other transport processes, such as hyperpycnal flows or turbidity currents  
341 were common in the system, the biogenic destruction removed all the evidence. Following the  
342 MacEachern and Pemberton (1992) characterization, the Bardas Blancas system would therefore  
343 fall in the low-energy category of the storm-influenced shoreface systems.

344 Thick monotonous successions (>100 m-thick) of storm-influenced, shallow-marine deposits  
345 formed by persistent combination of processes that resulted in highly bioturbated strata are not  
346 common in the stratigraphic record, but they tend to be restricted to certain geological conditions  
347 (Figs. 10, 11; Table 2). The Upper Jurassic Farsund Formation in the Norwegian Central Graben (distal  
348 equivalent of the Ula Formation, Bergan et al., 1989; Fraser et al., 2003), the Upper Jurassic Heather  
349 and Lower Kimmeridge Clay formation in the UK Central Graben (distal equivalents of the Fulmar

350 Formation, Donovan et al., 1993; Gowland, 1996), and the transition from the Middle Jurassic  
351 Tarbert to Heather Formations in the North Viking Graben (Råvnas et al., 1997; Råvnas and Steel,  
352 1998; Løseth et al., 2009) are all subsurface examples showing facies and bioturbation patterns that  
353 are remarkably similar to the ones observed in outcrops and subsurface for the Bardas Blancas  
354 Formation (Fig. 10D). The Early to Middle Jurassic Bridport Sand Formation in the Wessex Basin  
355 (Morris et al., 2006) and the Late Cretaceous Emery Sandstone Member of the Mancos Shale  
356 (Edwards et al., 2005), are partial or total exhumed examples of highly bioturbated shallow-marine  
357 successions.

358 Strata of the Farsund Formation in the Norwegian Central Graben are dominated by intensely  
359 bioturbated muddy sandstones and sandy mudstones that reach 200 m of thickness in Well 2/1-6  
360 (Fig. 10A). The more proximal equivalent Ula Formation is mostly composed of highly bioturbated  
361 sandstones, overall characterized as reflecting the weak to moderate shoreface profiles (Baniak et  
362 al., 2014, 2015) following the model from MacEachern and Pemberton (1992). The sedimentology  
363 and ichnology of the Fulmar Formation in the UK Central Graben has been reported in detail by  
364 Howell et al. (1996) and Gowland (1996). They concur on the long-lived development of a storm-  
365 influenced shoreface-offshore system, in which biogenic complete destruction of depositional  
366 structures largely prevailed in lower shoreface and offshore-transition settings (Fig. 10B). As in the  
367 Ula Formation example, total bioturbation in the offshore transition zone of the Fulmar Formation  
368 was interpreted as the result of low magnitude and/or low frequency of storm events (Howell et al.,  
369 1996). Collectively, these Upper Jurassic units of the Central Graben developed in a rifting tectonic  
370 stage and show long-term (several million years) aggradational to retrogradational stacking patterns  
371 (Howell et al., 1996; Mannie et al., 2014; 2016) (Fig 11).

372 The facies association and stacking patterns of the Tarbert and Lower Heather succession, in  
373 the North Viking Graben, were described by Løseth et al. (2009), based on cores and several key  
374 wells including well 30/9-14 (Fig. 10C). In this well the gamma-ray log for most of the Lower Heather  
375 interval suggests very uniform response, whereas cores display relatively homogenous, highly  
376 bioturbated muddy sandstones (Fig. 10C) grading to bioturbated sandstones with little preservation  
377 of HCS-beds. This uppermost succession has been interpreted to represent a parasequence with  
378 progradation from offshore, into offshore-transition settings and lowermost shoreface, within a  
379 long-term retrogradational stacking pattern (Løseth et al., 2009) (W3 in Fig. 11). As suggested by the  
380 authors, bioturbation intensity increases from W2 to W3 within the retrogradational stacking

381 pattern (Løseth et al., 2009, their figure 4). This net transgressive trend was developed within a  
382 synrift setting during the Bathonian and probably lasted 1-2 Ma (Mannie et al., 2016).

383 The Early to Middle Jurassic Bridport Sand Formation in the Wessex Basin (UK) is another  
384 example of storm-influenced, intensely bioturbated succession (Morris et al., 2006). According to  
385 the high degree of biogenic reworking, the dominant siltstones and silty sandstones with uncommon  
386 preserved storm beds were interpreted as reflecting low-energy lower-shoreface and offshore-  
387 transition settings (Morris et al., 2006). Interestingly, no evidence of nearby river influence or river-  
388 mouth processes were recorded, and sand supply to the shoreface settings was related to along-  
389 shore transport. Moreover, a well-defined, long-term aggradational stacking pattern was defined  
390 for the unit in extensional fault-bounded depocentres, and related to localized, relatively higher  
391 tectonic subsidence (Morris et al., 2006) (Table 2). One fully exhumed example of thick, highly  
392 bioturbated storm-influenced shallow-marine successions occurs within Late Cretaceous strata of  
393 the Book Cliffs, Utah (USA). The Emery Sandstone Member of the Mancos Shale is up to 250 m and  
394 represents the aggradational stack of storm-dominated shoreface parasequences developed in a  
395 foreland basin setting (Edwards et al., 2005) (Table 2).

396 All of these examples suggest that the Bardas Blancas Formation is a good analogue for thick  
397 bioturbated shallow-marine successions occurring in a variety of basinal settings, but preferentially  
398 in those having storm-surges as main across-offshore transport process in relatively confined or  
399 small depocentres, low to moderate riverine influence and a long-term balance between sediment  
400 supply and accommodation (i.e., aggradational stacking patterns) (Fig 11). Thus, it seems an  
401 oversimplification to assume that these basin conditions would be overruled by the frequency and  
402 magnitude of atmospheric processes (i.e. storms), which would also vary significantly across the  
403 long time periods some of these successions encompass.

404

## 405 **6.2. Possible controls on thick bioturbated storm-influenced shallow-marine successions**

406 Based on the occurrence of similar, thick storm-generated shallow-marine successions  
407 sharing more geological attributes than just their highly bioturbated nature, we propose to relate  
408 the total destruction of original storm beds and sedimentary structures over several million years  
409 to a suite of factors, rather than assuming that what they have in common is just a similar frequency  
410 and/or magnitude of atmospheric processes (i.e., storms).

411 Firstly, most of the examples discussed above (section 6.1) are related to complex syn-rift or  
412 early post-rift topography that define relative small depocentres during long-term marine  
413 transgressions (Howell et al., 1996; Veiga et al., 2013). These depocentres were mostly elongated  
414 and a few kms to 10s of kms wide (Fig. 11). It would be possible to relate this depositional context  
415 to the ability of the benthic fauna to recolonize almost the entire extent of these small depocentres,  
416 to produce not only total vertical bioturbation (as seen in 1D cores, Fig. 10), but also generating  
417 destruction of original beds for several kilometers laterally, as recorded in the outcrops of the Bardas  
418 Blancas Formation. In other words, we relate the relatively small size of the depositional setting to  
419 the high efficiency of re-colonization fauna to destroy most of the individual storm deposits,  
420 independently of how fast new colonization occurred, or the storm recurrence (or frequency). This  
421 destruction efficiency is steadily high across the recorded segments of the depositional environment  
422 (from the lower shoreface to proximal offshore), and does not necessarily follow the trend observed  
423 in modern shelves, in which the degree of bioturbation decreases in an offshore direction (Snedden  
424 and Nummedal, 1991). Howell et al. (1996) already used this basin-scale factor to support their  
425 process-realistic depositional model for the bioturbated, sand-dominated deposits of the Fulmar  
426 Formation. Moreover, Morris et al. (2006) suggested that small areas of accumulation in the  
427 Bridport Formation could have been more prone to extensive biotic proliferation, increasing the  
428 destruction success of storm-event beds. Going further, it could be speculated that the relatively  
429 small size of depocentres would allow a more homogenous distribution of the food source for the  
430 benthic fauna, which would ultimately account for its success in re-colonizing the entire depositional  
431 setting at all times.

432 An additional, long-term control on these thick bioturbated successions is related to the  
433 potential riverine influence (i.e., water and sediment input) to the marine realm. Modern studies  
434 have shown that individual, hurricane-related storm-event beds have high probability to be  
435 completely destroyed by bioturbation when riverine influence is relatively low and water depth is  
436 shallow (< 30 m), for example in the Texas inner shelf (Snedden and Nummedal, 1991). Likewise, it  
437 has also been recently demonstrated that amalgamated storm beds can be biogenically destroyed  
438 fairly rapidly (< 10 years) under conditions of high riverine influence, such as several hurricane-event  
439 layers described immediately downdrift of the Mississippi River delta in similar water depths (Walsh  
440 et al., 2018). The stratigraphic record of the intensely bioturbated succession reported in our study  
441 suggests a sustained biogenic destruction efficiency close to 100% during several million years (Fig.  
442 11). It follows that stress factors for benthic fauna typically associated with nearby, high riverine



443 influence (such as high turbidity or significant salinity fluctuations) were short-lived or uncommon  
444 episodes in the reported depositional settings. Therefore, for most of the Bardas Blancas Formation  
445 we infer a low riverine influence, with poorly integrated fluvial systems and significant along-shore  
446 sand supply. This seems to be the case for other examples discussed in section 6.1 and shown in  
447 Table 2. Howell et al. (1996) inferred absence of large deltas and poorly developed fluvial systems  
448 as clastic suppliers to the marine sandstones of the Fulmar Formation, whereas Morris et al. (2006)  
449 related the highly bioturbated succession to the lack of nearby river-mouth processes and significant  
450 along-shore transport. The intensely bioturbated Emery Member was also related to a moment of  
451 small rivers draining the Sevier Orogen, rather than a large integrated fluvial system as inferred for  
452 the shoreface settings of its underlying and overlying units (Edwards et al., 2005).

453 Another evident similarity between all the aforementioned examples is associated with the  
454 long-term stacking pattern (Fig. 11). The early post-rift Bardas Blancas Formation and the rift to early  
455 post-rift successions of the Central Graben show a consistent aggradational to retrogradational  
456 stacking involving ca. 7 to 20 Myr (Fig. 11) (Table 2). The transition from the fluvial to estuarine  
457 deposits of the Tarbert Formation, and then into the marine deposits of the lower Heather  
458 Formation, represents first a net retrogradational trend that becomes more aggradational-to-  
459 retrogradational (W2 and W3, Fig 11). Interestingly, the overall bioturbation index in the offshore-  
460 transition deposits increases in the W3 interval (Løseth et al., 2009), suggesting the maximum  
461 destruction efficiency of storm-event beds occurred at that time. The Emery Sandstone succession  
462 represents another unusual record of long-term aggradational stacking pattern (ca. 1.7 Myr, Table  
463 2), in which the sedimentation rates were low compared to those of underlying and overlying units  
464 (Edwards et al, 2005). Coincidentally, the offshore-transition to lower-shoreface deposits of the Emery  
465 Sandstone reflect one of the highest destruction efficiency of storm-event beds in the Upper  
466 Cretaceous record of the Wasatch-Book Cliff section. This shows a marked difference with less  
467 bioturbated, environment-equivalent deposits, for example the younger Kenilworth Member (Eide  
468 et al., 2015) and the Grassy Member (Onyeonu et al., 2018) of the Blackhawk Formation, both units  
469 developed in progradational stacking patterns. Thus, a delicate long-lived balance between  
470 sediment supply and accommodation to create thick successions with highly aggradational (to  
471 slightly retrogradational) stacking patterns could be linked to sedimentation rates across the  
472 shoreface-offshore system. The offshore-transition and proximal offshore sectors of the system  
473 would have experienced low net sedimentation rates that -- if all other variables remained fairly  
474 constant-- would have produced a similar effect than low frequency of storm-surge flows reaching

475 those regions. The lack of significant progradational events (basinward facies shifts) also contributed  
476 to create thick, fairly homogenous strata, without major sedimentation breaks or sequence  
477 boundaries, and representing one or two segments of the depositional system. In the case of the  
478 investigated examples those segments correlated approximately with areas below the fair weather  
479 wave base and storm wave base, in which the highest destruction efficiency of storm-event beds  
480 took place.

481 In summary, by combining the observations and interpretations of different thick, intensely  
482 bioturbated, shallow-marine successions we dispute the common assumption that the final  
483 bioturbated product can be associated to low frequency or low magnitude of storms. Alternatively,  
484 we propose that the long-lived efficiency of benthic fauna on destroying most if not all the storm-  
485 event beds (that reached the offshore transition sector), results from the combination of two or  
486 three factors: deposition in relatively confined marine depocentres, persistent low riverine  
487 influence, and/or a long-term, aggradational to slightly retrogradational stacking pattern. As these  
488 conditions can be recreated in a variety of basin styles, such as rift, early post-rift, and foreland  
489 settings, the recognition of thick, bioturbated successions as the ones discussed here can be used  
490 to infer more realistic constrains for depositional models and better predict facies distribution in  
491 these storm-influenced systems.

492

## 493 **7. CONCLUSIONS**

494 1 - The Lower-Middle Jurassic Bardas Blancas Formation represents a thick (up to 230 m), highly  
495 bioturbated, storm-influenced shallow-marine succession developed during the early post-rift  
496 stage of the Neuquén Basin.

497 2 - Most of its stratigraphic record is dominated by muddy sandstones and sandy to silty mudstones  
498 deposited in offshore-transition to proximal-offshore settings, in which benthic- fauna efficiency  
499 to destroy individual storm-event beds was persistently close to 100 % during a time span  
500 ranging from 7 to 10 Myr. This highly efficient biogenic reworking was mostly associated to  
501 deposit-feeder organisms of the *Cruziana* ichnofacies.

502 3 - The Bardas Blancas Formation shears several attributes with other thick (> 100 m) intensely  
503 bioturbated successions including: deposition in relatively confined marine depocentres,  
504 persistent low riverine influence, and long-term (2- 20 Myr) aggradational stacking pattern. Yet,

505 all these biogenically reworked successions are developed in a variety of structural styles,  
506 including rift, early post-rift, and foreland settings.

507 4 - We question the assumption that the resulting architecture of these unusual thick, bioturbated  
508 shoreface-offshore successions at different scales should be directly associated to low frequency  
509 or low magnitude of storms. Alternatively, we propose that the long-lived efficiency of benthic  
510 fauna on destroying almost all the storm-event beds accumulated in these depositional  
511 environments during several million years was more likely controlled by the co-occurrence of the  
512 following depositional factors: a) relatively small depocenters with infaunal colonization evenly  
513 distributed in intermediate to distal sectors of the marine system, b) benthic fauna very rarely  
514 affected by physico-chemical stress factors in those regions due to overall low riverine influence,  
515 and c) delicate balance between sediment supply and accommodation producing relatively low  
516 net sedimentation rates across the system.

517 5 - These depositional conditions can be recreated in a variety of basin styles, so the results of this  
518 contribution on the controls of thick, highly bioturbated successions can be used to infer more  
519 realistic constrains for depositional models and better predict facies distribution in these distinct  
520 storm-influenced systems.

521

## 522 **ACKNOWLEDGMENTS**

523 E.S. would like to thank CONICET and Universidad Nacional de La Plata for partially supporting this  
524 project. M.P. and I.M. acknowledge Aker BP, sponsor of the ShelfSed project (University of Oslo).

525

## 526 **REFERENCES**

527 Aigner, T., 1982. Calcareous tempestites: storm-dominated stratification in upper Muschelkalk  
528 limestones (Middle Trias, SW-Germany), in: Einsele, G., Seilacher, A. (Eds.), *Cyclic and Event*  
529 *Stratification*: Berlin (Springer-Verlag), pp. 180-198.

530 Arregui, C., Carbone, O., Martínez, R., 2011. El Grupo Cuyo (Jurásico Temprano-Medio) en la Cuenca  
531 Neuquina, Geología y Recursos Naturales de la Provincia del Neuquén: Buenos Aires, Relatorio del  
532 18 Congreso Geológico Argentino, pp. 77-89.

533 Baniak, G.M., Gingras, M.K., Burns, B.A., George Pemberton, S., 2014. An example of a highly  
534 bioturbated, storm-influenced shoreface deposit: Upper Jurassic Ula Formation, Norwegian North  
535 Sea. *Sedimentology* 61, 1261-1285.

536 Baniak, G.M., Gingras, M.K., Burns, B.A., Pemberton, S.G., 2015. Petrophysical Characterization of  
537 Bioturbated Sandstone Reservoir Facies In the Upper Jurassic Ula Formation, Norwegian North Sea,  
538 Europe. *Journal of Sedimentary Research* 85, 62-81.

539 Bergan, M., Tørudbakken, B., Wandås, B., 1989. Lithostratigraphic correlation of Upper Jurassic  
540 sandstones within the Norwegian Central Graben: sedimentological and tectonic implications, in:  
541 Collinson, J.D. (Ed.), *Correlation in Hydrocarbon Exploration*. Springer Netherlands, Dordrecht, pp.  
542 243-251.

543 Burgess, P.M., Flint, S., Johnson, S., 2000. Sequence stratigraphic interpretation of turbiditic strata:  
544 An example from Jurassic strata of the Neuquén basin, Argentina. *GSA Bulletin* 112, 1650-1666.

545 D'Elia, L., Bilmes, A., Franzese, J.R., Veiga, G.D., Hernández, M., Muravchik, M., 2015. Early evolution  
546 of the southern margin of the Neuquén Basin, Argentina: Tectono-stratigraphic implications for rift  
547 evolution and exploration of hydrocarbon plays. *Journal of South American Earth Sciences* 64, 42-  
548 57.

549 Donovan, A.D., Djacic, A.W., Ioannides, N.S., Garfield, T.R., Jones, C.R., 1993. Sequence stratigraphic  
550 control on Middle and Upper Jurassic reservoir distribution within the UK Central North Sea.  
551 *Geological Society, London, Petroleum Geology Conference series* 4, 251-269.

552 Doyle, P., Poiré, D.G., Spalletti, L.A., Pirrie, D., Brenchley, P., Matheos, S.D., 2005. Relative  
553 oxygenation of the Tithonian — Valanginian Vaca Muerta—Chachao formations of the Mendoza  
554 Shelf, Neuquén Basin, Argentina, in: Veiga, G., Spalletti, L., Howell, J., Schwarz, E. (Eds.), *The*  
555 *Neuquén Basin: A Case Study in Sequence Stratigraphy and Basin Dynamics*. Geological Society,  
556 London, Special Publications, 252, pp. 185-206.

557 Dumas, S., Arnott, R.W.C., 2006. Origin of hummocky and swaley cross-stratification— The  
558 controlling influence of unidirectional current strength and aggradation rate. *Geology* 34, 1073-  
559 1076.

560 Edwards, C.M., Howell, J.A., Flint, S.S., 2005. Depositional and Stratigraphic Architecture of the  
561 Santonian Emery Sandstone of the Mancos Shale: Implications for Late Cretaceous Evolution of the  
562 Western Interior Foreland Basin of Central Utah, U.S.A. *Journal of Sedimentary Research* 75, 280-  
563 299.

564 Eide, C.H., Howell, J.A., Buckley, S.J., 2015. Sedimentology and reservoir properties of tabular and  
565 erosive offshore transition deposits in wave-dominated, shallow-marine strata: Book Cliffs, USA.  
566 *Petroleum Geoscience* 21, 55-73.

567 Franzese, J.R., Spalletti, L.A., 2001. Late Triassic–early Jurassic continental extension in  
568 southwestern Gondwana: tectonic segmentation and pre-break-up rifting. *Journal of South*  
569 *American Earth Sciences* 14, 257-270.

570 Franzese, J.R., Veiga, G.D., Schwarz, E., Gómez-Pérez, I., 2006. Tectonostratigraphic evolution of a  
571 Mesozoic graben border system: the Chachil depocentre, southern Neuquén Basin, Argentina.  
572 *Journal of the Geological Society* 163, 707-721.

573 Fraser, S.I., Robinson, A.M., Johnson, H.D., Underhill, J.R., Kadolsky, D.G.A., Connell, R., Johannesen,  
574 P., Ravnås, R., 2003. Upper Jurassic, in: Evans, D., Graham, C., Armour, A., Bathurst, P. (Eds.), *The*  
575 *Millennium Atlas: Petroleum Geology of the Central and Northern North Sea*. The Geological Society  
576 of London, London, UK, pp. 157-189.

577 Giambiagi, L., Tunik, M., Barredo, S., Bechis, F., Ghiglione, M., Alvarez, P., Drosina, M., 2009.  
578 *Cinemática de apertura del sector norte de la cuenca Neuquina*. *Revista de la Asociación Geológica*  
579 *Argentina* 65, 278-292.

580 Gowland, S., 1996. Facies characteristics and depositional models of highly bioturbated shallow  
581 marine siliciclastic strata: an example from the Fulmar Formation (Late Jurassic), UK Central Graben.  
582 Geological Society, London, Special Publications 114, 185-214.

583 Gulisano, C.A., 1981. El Ciclo Cuyano en el norte de Neuquén y sur de Mendoza, Congreso Geológico  
584 Argentino, pp. 579-592.

585 Gulisano, C.A., Gutiérrez Pleimling, A.R., Digregorio, R.E., 1984. Esquema estratigráfico de la  
586 secuencia jurásica del oeste de la provincia del Neuquén, Congreso Geológico Argentino, pp. 236-  
587 259.

588 Gulisano, C., Gutiérrez Pleimling, A., 1994. The Jurassic of the Neuquén Basin, a) Neuquén Province-  
589 Field Guide. Asociación Geológica Argentina, Serie E2, Buenos Aires, Argentina.

590 Hodgson, D., Brooks, H.L., Ortiz-Karpf, A., Sychala, Y., Lee, D.R., Jackson, C.A., 2018. Entrainment  
591 and abrasion of megaclasts during submarine landsliding and their impact on flow behaviour.  
592 Geological Society, London, Special Publications, 477, 223-240.

593 Hampson, G.J., 2000. Discontinuity Surfaces, Clinoforms, and Facies Architecture in a Wave-  
594 Dominated, Shoreface-Shelf Parasequence. *Journal of Sedimentary Research* 70, 325-340.

595 Howell, J.A., Flint, S.S., 1996. A model for high resolution sequence stratigraphy within extensional  
596 basins. Geological Society, London, Special Publications 104, 129-137.

597 Howell, J.A., Schwarz, E., Spalletti, L.A., Veiga, G.D., 2005. The Neuquén Basin: an overview.  
598 Geological Society, London, Special Publications 252, 1-14.

599 Isla, M.F., Coronel, M., Schwarz, E., Veiga G.D., 2020. Depositional architecture of a wave-dominated  
600 clastic shoreline (Pilmatué Member, Argentina): improving knowledge about the preservation of  
601 bar-trough systems. *Marine and Petroleum Geology*. doi: 10.1016/j.marpetgeo.2020.104417.

602 Legarreta, L., Uliana, M.A., 1991. Jurassic—Marine Oscillations and Geometry of Back-Arc Basin Fill,  
603 Central Argentine Andes, in: Macdonald, D.I.M. (Ed.), *Sedimentation, Tectonics and Eustasy:*  
604 *Sedimentation, Tectonics and Eustasy: Sea-Level Changes at Active Margins*. Blackwell Scientific, pp.  
605 429-450.

606 Legarreta, L., Uliana, M.A., 1996. The Jurassic succession in west-central Argentina: stratal patterns,  
607 sequences and paleogeographic evolution. *Palaeogeography, Palaeoclimatology, Palaeoecology*  
608 120, 303-330.

609 Løseth, T.M., Ryseth, A.E., Young, M., 2009. Sedimentology and sequence stratigraphy of the middle  
610 Jurassic Tarbert Formation, Oseberg South area (northern North Sea). *Basin Research* 21, 597-619.

611 MacEachern, J.A., Bann, K.L., 2008. The Role of Ichnology in Refining Shallow Marine Facies Models,  
612 in: Hampson, G.J., Steel, R.J., Burgess, P.M., Dalrymple, R.W. (Eds.), *Recent Advances in Models of*  
613 *Siliciclastic Shallow-Marine Stratigraphy*. SEPM Society for Sedimentary Geology, p. 0.

614 MacEachern, J.A., Pemberton, S.G., 1992. Ichnological Aspects of Cretaceous Shoreface Successions  
615 and Shoreface Variability in the Western Interior Seaway of North America, *Applications of*  
616 *Ichnology to Petroleum Exploration*, pp. 57-84.

617 MacEachern, J.A., Pemberton, S.G., Bann, K.L., Gingras, M.K., 2007. Departures from the Archetypal  
618 Ichnofacies: Effective Recognition of Physico-Chemical Stresses in the Rock Record, in: MacEachern,  
619 J.A., Bann, K.L., Gingras, M.K., Pemberton, S.G. (Eds.), *Applied Ichnology*. SEPM Society for  
620 *Sedimentary Geology, Short Course Notes* 52, pp. 65-93.

621 MacEachern, J.A., Zaitlin, B.A., Pemberton, S.G., 1999. A sharp-based sandstone of the Viking  
622 Formation, Joffre Field, Alberta, Canada; criteria for recognition of transgressively incised shoreface  
623 complexes. *Journal of Sedimentary Research* 69, 876-892.

624 Mannie, A.S., Jackson, C.A.-L., Hampson, G.J., 2014. Structural controls on the stratigraphic  
625 architecture of net-transgressive shallow-marine strata in a salt-influenced rift basin: Middle-to-  
626 Upper Jurassic Egersund Basin, Norwegian North Sea. *Basin Research* 26, 675-700.

627 Mannie, A.S., Jackson, C.A.-L., Hampson, G.J., Fraser, A.J., 2016. Tectonic controls on the spatial  
628 distribution and stratigraphic architecture of a net-transgressive shallow-marine synrift succession  
629 in a salt-influenced rift basin: Middle to Upper Jurassic, Norwegian Central North Sea. *Journal of the*  
630 *Geological Society* 173, 901-915.

631 Morris, J.E., Hampson, G.J., Johnson, H.D., 2006. A sequence stratigraphic model for an intensely  
632 bioturbated shallow-marine sandstone: the Bridport Sand Formation, Wessex Basin, UK.  
633 *Sedimentology* 53, 1229-1263.

634 Niedoroda, A.W., Swift, D.J.P., Thorne, J.A., 1989. Modeling shelf storm beds: controls of bed  
635 thickness and bedding sequence, in: Morton, R.A., Nummedal, D. (Eds.), *Shelf sedimentation, shelf*  
636 *sequences and related hydrocarbon accumulation*. Proceedings of the 17th annual research  
637 conference, Gulf Coast Section. Society of Economic Paleontologists and Mineralogists Foundation,  
638 pp. 15-39.

639 Onyenanu, G.I., Jacquemyn, C.E.M.M., Graham, G.H., Hampson, G.J., Fitch, P.J.R., Jackson, M.D.,  
640 2018. Geometry, distribution and fill of erosional scours in a heterolithic, distal lower shoreface  
641 sandstone reservoir analogue: Grassy Member, Blackhawk Formation, Book Cliffs, Utah, USA.  
642 *Sedimentology* 65, 1731-1760.

- 643 Pemberton, S.G., MacEachern, J.A., Dashtgard, S.E., Bann, K.L., Gingras, M.K., Zonneveld, J.-P., 2012.  
644 Shorefaces, Trace Fossils as Indicators of Sedimentary Environments, pp. 563-603.
- 645 Privat, A., Hodgson, D.M., Jackson, C.A.-L., Schwarz, E., Peakall, J., accepted. Evolution from syn-rift  
646 carbonates to early post-rift deep-marine intraslope lobes: the role of rift basin physiography on  
647 sedimentation patterns. *Sedimentology*.
- 648 Ravnås, R., Bondevik, K., Helland-Hansen, W., Lømo, L., Ryseth, A., Steel, R.J., 1997. Sedimentation  
649 history as an indicator of rift initiation and development: the late Bajocian-Bathonian evolution of  
650 the Oseberg-Brage area, northern North Sea. *Norsk Geologisk Tidsskrift* 77, 205-232.
- 651 Ravnås, R., Steel, R.J., 1998. Architecture of Marine Rift-Basin Successions. *AAPG Bulletin* 82, 110-  
652 146.
- 653 Reading, H.G., Collinson, J.D., 1996. Clastic coasts, in: Reading, H.G. (Ed.), *Sedimentary*  
654 *Environments: Processes, Facies and Stratigraphy*. Blackwell Science, pp. 154-231.
- 655 Riccardi, A.C., 2008. El Jurásico de la Argentina y sus amonites. *Revista de la Asociación Geológica*  
656 *Argentina* 63, 625-643.
- 657 Sagripanti, L., Folguera, A., Giménez, M., Vera, E.R., Fabiano, J., Molnar, N., Fennell, L., Ramos, V.A.,  
658 2014. Geometry of Middle to Late Triassic extensional deformation pattern in the Cordillera del  
659 Viento (Southern Central Andes): A combined field and geophysical study. *Journal of Iberian Geology*  
660 40, 349-366.
- 661 Schwarz, E., Veiga, G.D., Álvarez Trentini, G., Isla, M.F., Spalletti, L.A., 2018. Expanding the spectrum  
662 of shallow-marine, mixed carbonate–siliciclastic systems: Processes, facies distribution and  
663 depositional controls of a siliciclastic-dominated example. *Sedimentology* 65, 1558-1589.
- 664 Snedden, J.W., Nummedal, D., 1991. Origin and Geometry of Storm-Deposited Sand Beds in Modern  
665 Sediments of the Texas Continental Shelf, in: Swift, D.J.P., Oertel, G.F., Tillman, R.W., Thorne, J.A.  
666 (Eds.), *Shelf Sand and Sandstone Bodies*. International Association of Sedimentologists Special  
667 Publication, 14, pp. 283-308.
- 668 Spalletti, L.A., Parent, H., Veiga, G.D., Schwarz, E., 2012. Amonites y Bioestratigrafía del grupo Cuyo  
669 en la Sierra de Reyes (Cuenca Neuquina central, Argentina) y su significado secuencial. *Andean*  
670 *geology* 39, 464-481.
- 671 Taylor, A.M., Goldring, R., 1993. Description and analysis of bioturbation and ichnofabric. *Journal of*  
672 *the Geological Society* 150, 141-148.
- 673 Veiga, G.D., Schwarz, E., Spalletti, L.A., 2011. Análisis estratigráfico de la Formación Lotena  
674 (Calloviano superior-Oxfordiano inferior) en la Cuenca Neuquina Central, República Argentina:  
675 Integración de información de afloramientos y subsuelo. *Andean geology* 38, 171-197.
- 676 Veiga, G.D., Schwarz, E., Spalletti, L.A., Massafarro, J.L., 2013. Anatomy And Sequence Architecture  
677 of the Early Post-Rift In the Neuquén Basin (Argentina): A Response To Physiography and Relative  
678 Sea-Level Changes. *Journal of Sedimentary Research* 83, 746-765.

679 Vergani, G.D., Tankard, A.J., Belotti, H.J., Welsink, H.J., 1995. Tectonic evolution and paleogeography  
680 of the Neuquén Basin, Argentina, in: Tankard, A.J., Suárez Soruco, R., Welsink, H.J. (Eds.), Petroleum  
681 Basins of South America. AAPG Memoirs, 62, pp. 383-402.

682 Walker, R.G., Plint, A.G., 1992. Wave- and storm-dominated shallow marine systems, in: Walker  
683 R.G., Plint, A.G. (Eds.), Facies Models: response to sea level change. Geological Association of  
684 Canada, pp. 219-238.

685 Walsh, J.P., Corbett, D.R., Alexander, C.R., 2018. Source-to-sink sedimentation: insights from  
686 modern continental-margin system studies. 20th International Sedimentological Congress, 13-17th  
687 August 2018, Québec City, Canada. Poster presentation.

688 Wheatcroft, R.A., 1990. Preservation potential of sedimentary event layers. *Geology* 18, 843-845.

689

690

## 691 **FIGURES AND FIGURE CAPTIONS**

692 **Fig 1. A.** Map of the Neuquén Basin with approximate location (red square) of the study area (Fig.  
693 2). **B.** Paleogeographic reconstruction of the Neuquén Basin during the Jurassic – Early-Cretaceous.  
694 The onset of subduction on the western margin of Gondwana and the early development of the  
695 Andean arc led to development of a large triangular-shape epicontinental basin, partially connected  
696 to the proto-Pacific Ocean through a volcanic arc. Modified after Howell et al. (2005).

697 **Fig. 2.** Cross section (integrating outcrop and well data) showing the stratigraphic setting and overall  
698 depositional architecture of the early post-rift succession (Bardas Blancas, Los Molles and Lajas  
699 formations) in central Neuquén Basin, as well as the older Remoredo Formation (syn-rift  
700 volcanoclastic deposits) and Choiyoi Group (basement) units. Inset shows detailed map of the cross  
701 section. Modified from Veiga et al. (2013). Chronostratigraphy based on ammonite dating from  
702 Spalletti et al. (2012).

703 **Fig. 3. A.** Geologic map of the Sierra de Reyes region, showing the different locations studied in  
704 Veiga et al. (2013) (black stars) and this study (white stars). **B.** Satellite image of the study area, in  
705 the eastern flank of the Sierra de Reyes anticline, showing the location of the sections studied in  
706 the Cuyo Group.

707 **Fig. 4.** Field panoramas of Agua del Campo (**A**) and Agua de Heredia (**B**), showing the location of  
708 main stratigraphic units, and their bounding surfaces. **C.** Simplified stratigraphic section showing the  
709 overall aggradational-to-retrogradational stacking of the Bardas Blancas Formation, and its vertical  
710 relationships with the underlying and overlying lithostratigraphic units. Parasequence sets (PSS's)  
711 after Veiga et al. (2013).

712 **Fig. 5.** Outcrop examples of the different facies associations defined in this study. **A.** Cross-bedded,  
713 organic-rich and poorly-sorted pebbly to medium-grained sandstones (FA1- Delta Front).  
714 Parasequence Set I, Agua de Heredia. **B.** Amalgamated, trough cross-bedded, well-sorted fine-  
715 grained sandstones (FA2 – Upper shoreface). Parasequence Set I, Agua de Heredia. **C.** Tabular to



716 slightly undulate, medium-bedded fine-grained sandstones, with hummocky cross stratification  
717 (HCS) (FA3- Lower shoreface). Parasequence Set II, Agua del Campo. **D.** Moderate to highly  
718 bioturbated sandstones and muddy sandstones, with local preservation of HCS (FA4- Offshore  
719 transition). Parasequence Set II, Agua del Campo. **E.** Highly bioturbated sandy and silty mudstones,  
720 with subordinate muddy sandstones (FA5- Proximal offshore). Parasequence Set II, Agua de Heredia.  
721 **F.** Massive to crudely laminated gray mudstones with occasional diagenetic nodule-rich horizons  
722 (FA6- Distal offshore). Parasequence Set II, Agua de Heredia. See Table 1 for more details about their  
723 main attributes, and Figs. 2 and 4 for location in stratigraphy.

724 **Fig. 6.** Selected examples of trace fossils found in offshore transition (FA4) and proximal offshore  
725 (FA5) facies associations.

726 **Fig. 7.** General depositional model of the Bardas Blancas Formation in the study area, showing the  
727 distribution of different facies associations (FA's) and their associated depositional environments.  
728 Note the influence of inherited and under-filled rift topography in the stratigraphic architecture of  
729 early post-rift deposits. Not to scale.

730 **Fig. 8.** Examples of tabularity and bioturbation at different scales. **A.** Highly bioturbated, dm-scale  
731 muddy sandstones and sandy mudstones in offshore transition deposits (FA5). Parasequence Set III,  
732 Agua del Ñaco. **B.** Bioturbated offshore transition deposits (FA5), stacked in m-scale, well-defined  
733 bedsets. Parasequence Set III, Agua de Ñaco. **C.** General view of several m-scale bedsets, showing  
734 the homogeneous and tabular nature of the studied deposits. Parasequence Set II, Agua de Heredia.  
735 **D.** Stratigraphic section, containing the interval shown in **C**, with the lithological, sedimentary and  
736 bioturbation trends of a 10's of m-thick, shallowing-up succession (parasequence), made by several  
737 m-scale bedsets, and bounded by regional-scale flooding surfaces. Parasequence Set II, Agua de  
738 Heredia. See Figs. 2 and 4 for location in stratigraphy.

739 **Fig. 9.** Two examples of preserved HCS in storm-event beds. **A.** General view of the gradual vertical  
740 transition from proximal offshore (FA5) to offshore transition deposits (FA4). **B.** Example of partially  
741 preserved HCS in dominantly highly bioturbated proximal offshore deposits (FA5). Parasequence Set  
742 II, Agua de Heredia. **C.** Detail view of the contact between the fully bioturbated (*Chondrites*  
743 ichnofabric) upper part and the non-bioturbated lower part (preserving the original sedimentary  
744 structures) of the same event bed. Parasequence Set II, Agua de Heredia. **D.** Outcrop view of  
745 offshore transition deposits (FA4). **E.** Example of preserved HCS in a partially homogenized event  
746 bed, overlain and underlain by highly bioturbated muddy sandstones and sandy mudstones  
747 (offshore transition, FA4). Parasequence Set III, Agua del Campo Sur.

748 **Fig. 10.** GR well logs and core examples of highly bioturbated, storm-dominated shallow-marine  
749 successions comparable to the studied deposits. **A.** Upper Jurassic Farsund Formation, interpreted  
750 as the equivalent offshore transition deposits of the bioturbated, sand-rich Ula Formation in the  
751 Norwegian Central Graben. **B.** Heather and Intra-Heather Sandstone Formation, the offshore  
752 transition deposits overlying the transgressive shallow-marine sandstones of the Tarbert Formation,  
753 in Northern Viking Graben/Western Horda Platform. **C.** Heather Formation, also the equivalent  
754 offshore transition deposits of the highly bioturbated, Fulmar Formation, in the UK Central Graben.  
755 **D.** Lower-Middle Jurassic Bardas Blancas Formation, Neuquén Basin (this study).

756 **Fig. 11.** Structural setting, overall stratigraphic architecture and stacking pattern of the different  
757 highly bioturbated, storm-dominated shallow-marine successions shown in Fig. 10, and the Bardas  
758 Blancas Formation.

759

760 **Table 1.** Facies association classification, description and interpretation of the main processes and  
761 environments of deposition. Trace fossil content is listed in relative order of abundance. FWWB:  
762 Fair-weather wave base; SWWB: Storm-weather wave base.

763

764 **Table 2.** Main characteristics of the thick intensely bioturbated successions discussed in this  
765 contribution.

766

Figure 1

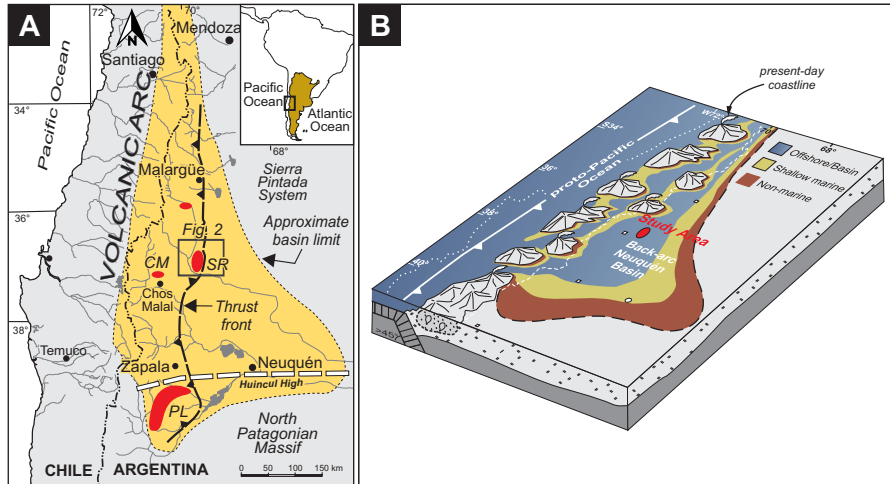
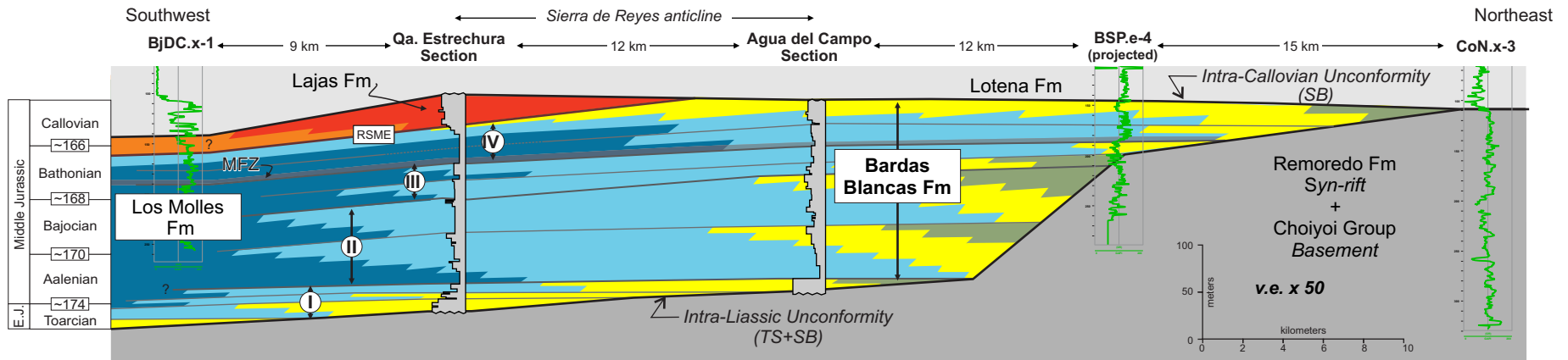


# Figure 2



- Coastal-plain deposits (inferred)
- Shoreface deposits
- Offshore-transition and upper offshore deposits
- Lower offshore deposits
- Deltaic deposits (proximal delta front to ?distal delta front)

- flooding surface bounding parasequence
- flooding surface bounding parasequence set
- II parasequence set I to IV
- MFZ maximum flooding zone
- RSME regressive surface of marine erosion
- TS Transgressive surface
- SB Sequence Boundary
- ~174 Stage boundary (Ma)

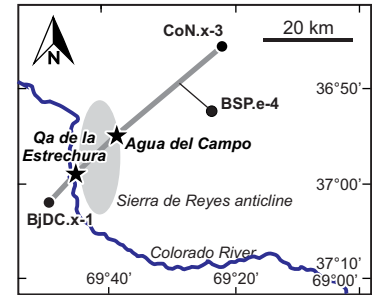


Figure 3

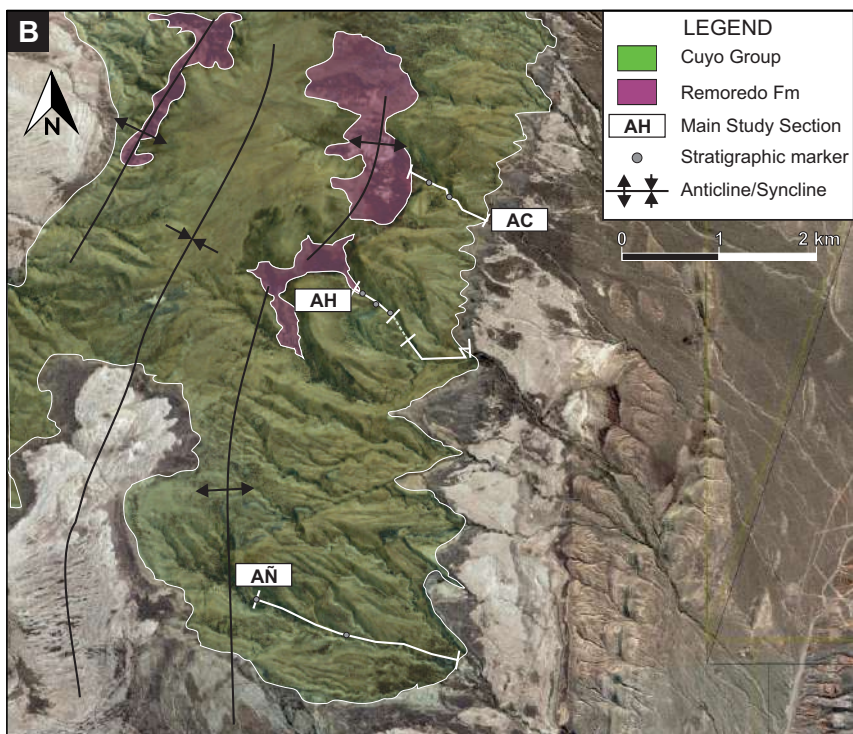
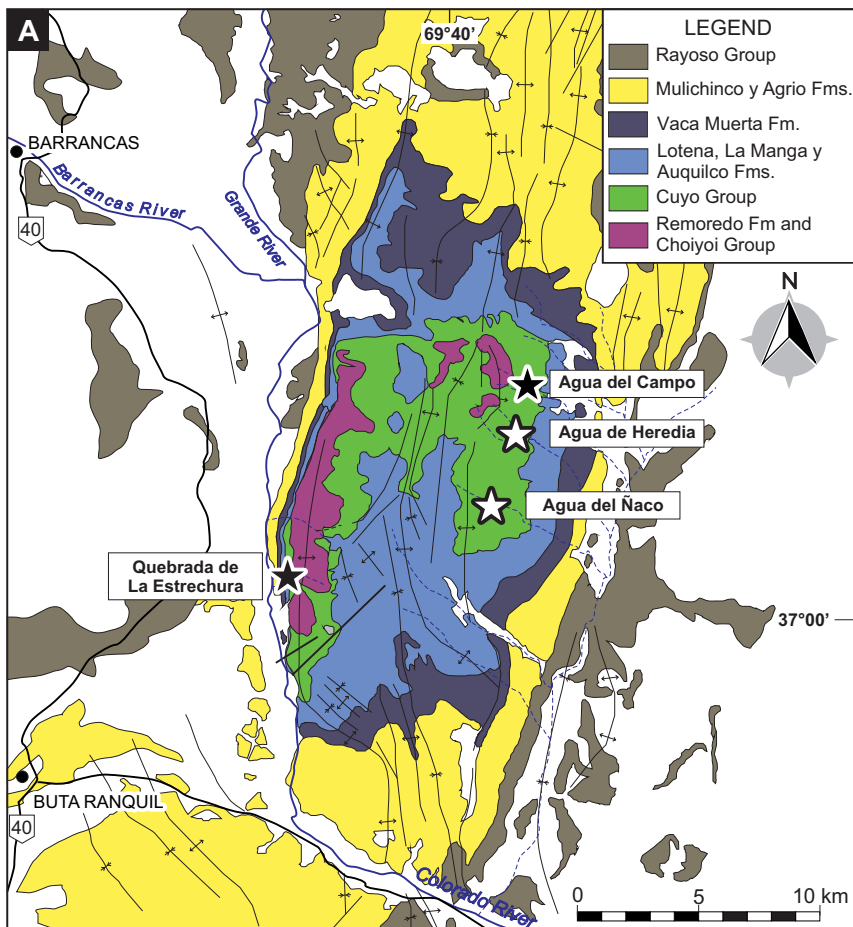


Figure 4

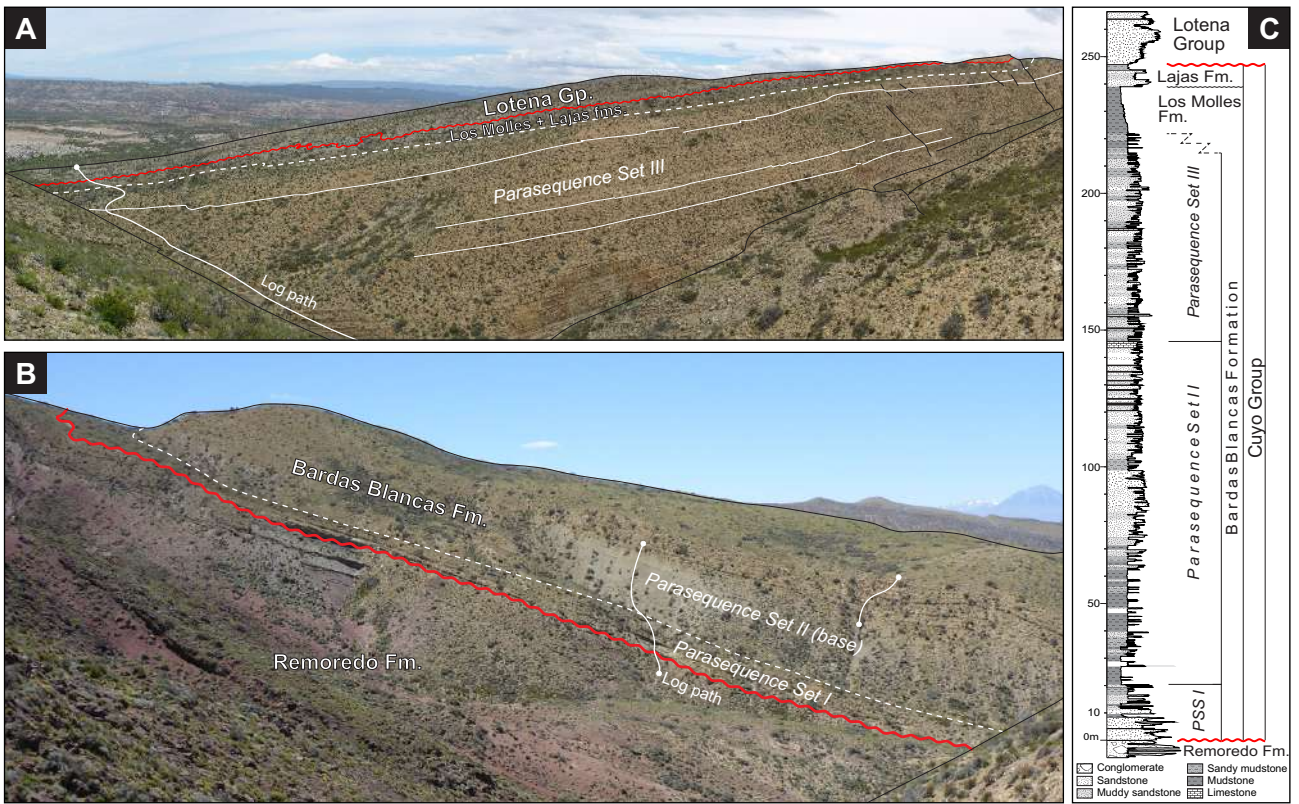




Figure 5



**Figure 06**

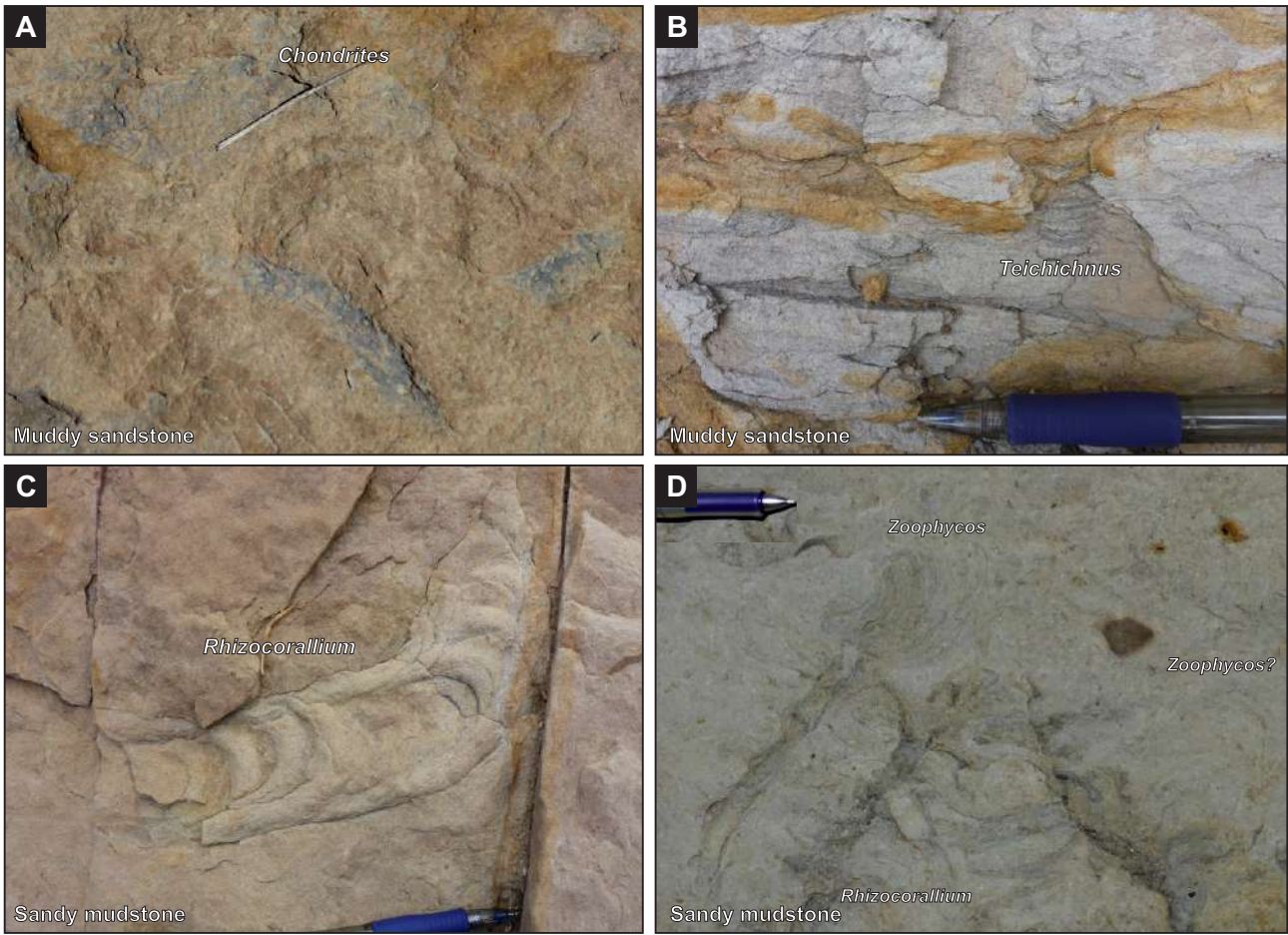




Figure 7

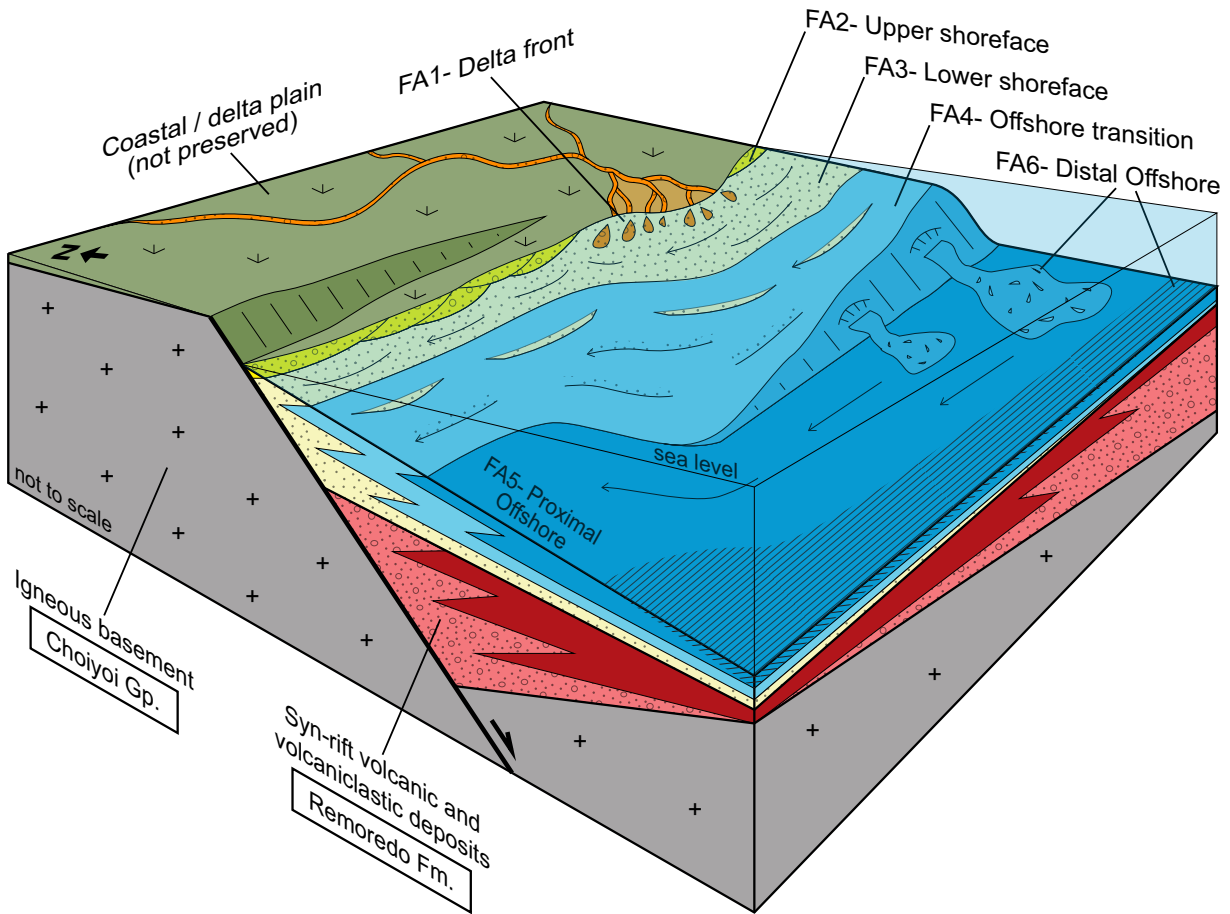


Figure 8

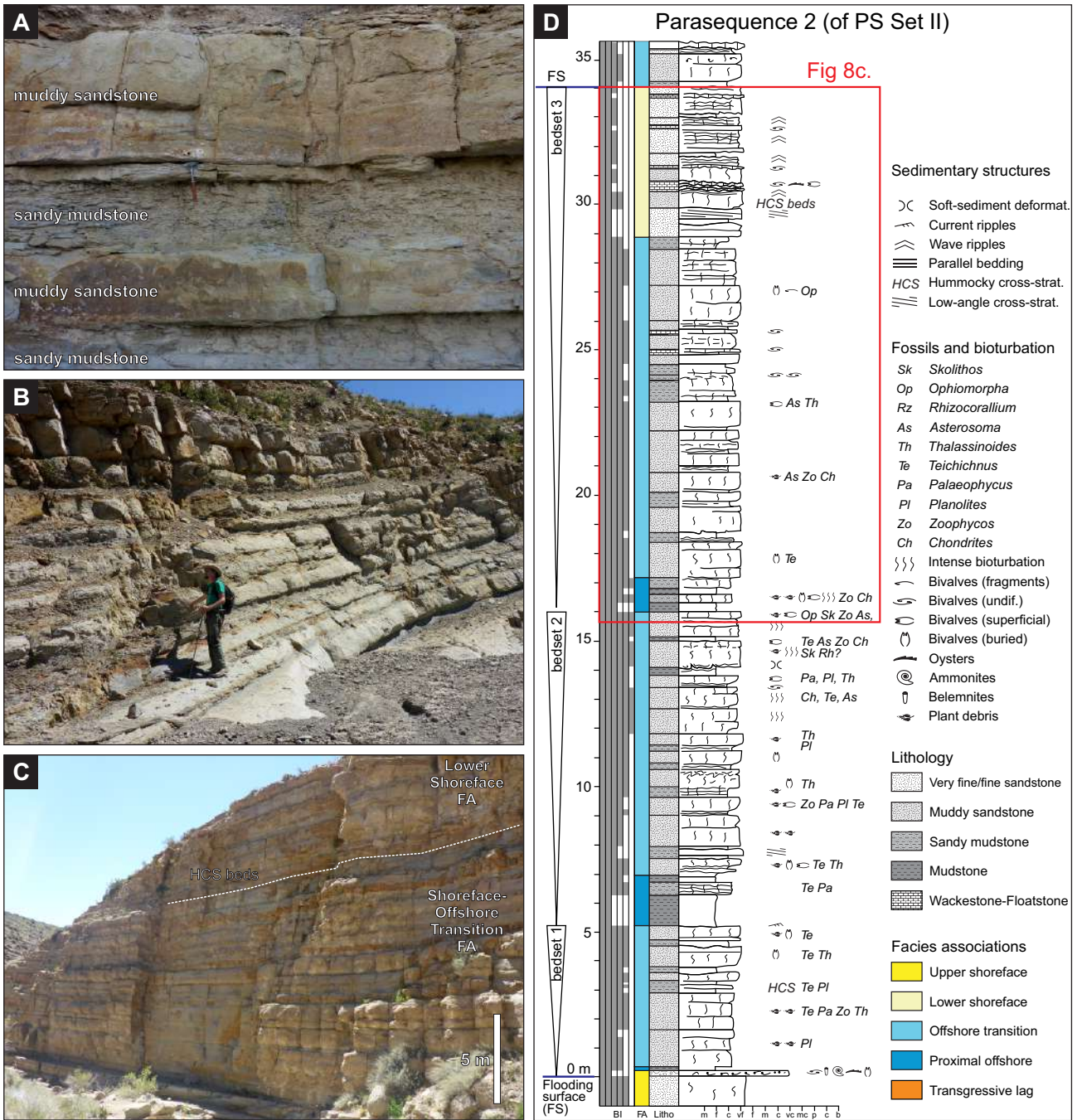
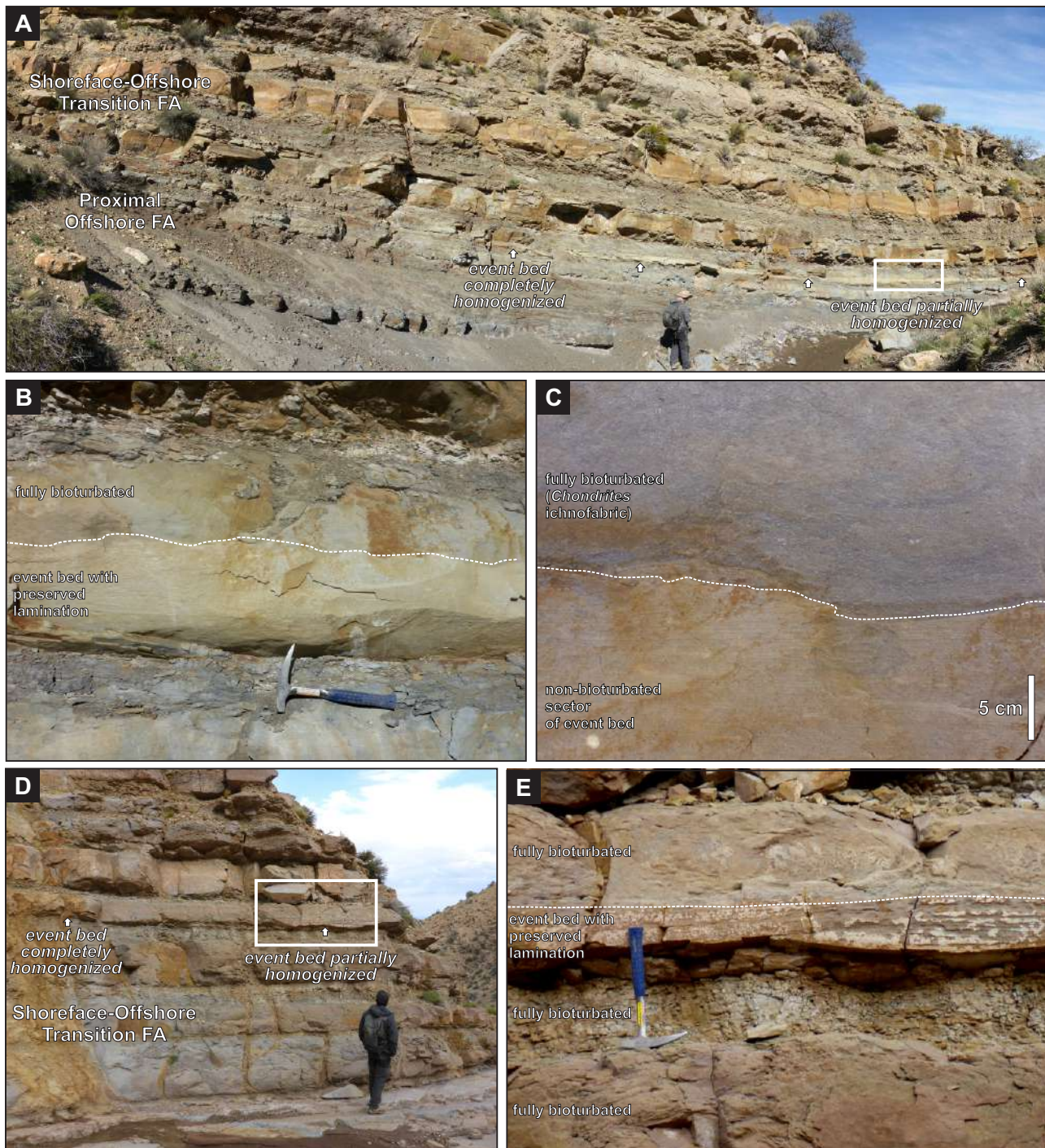


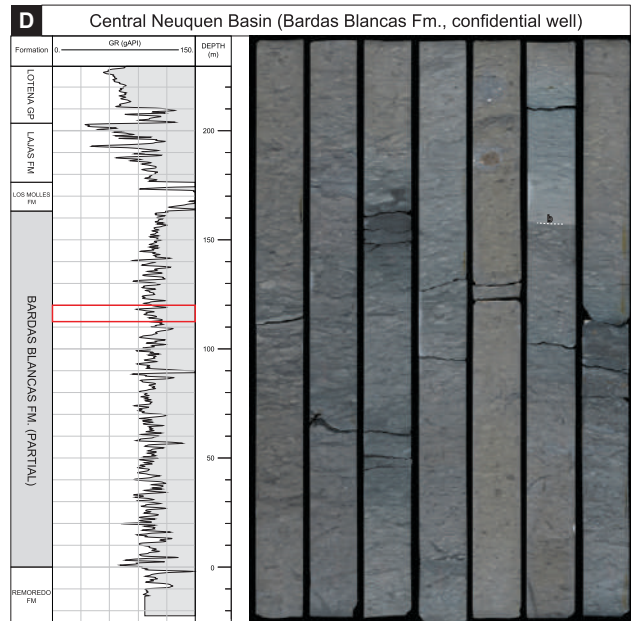
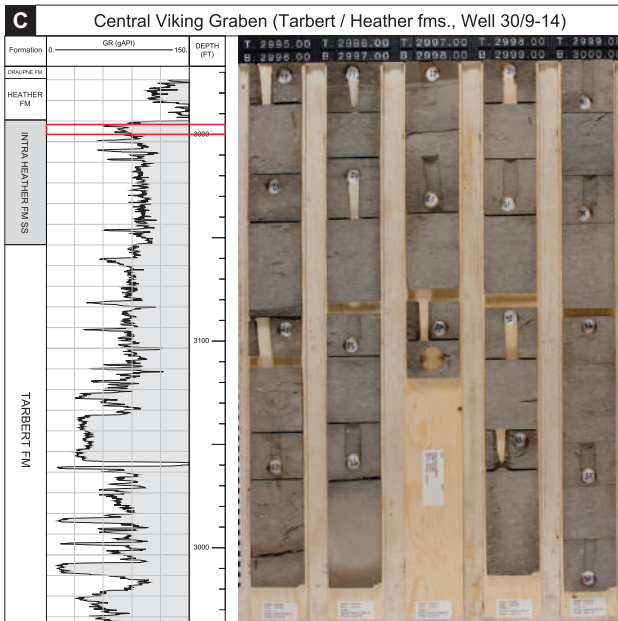
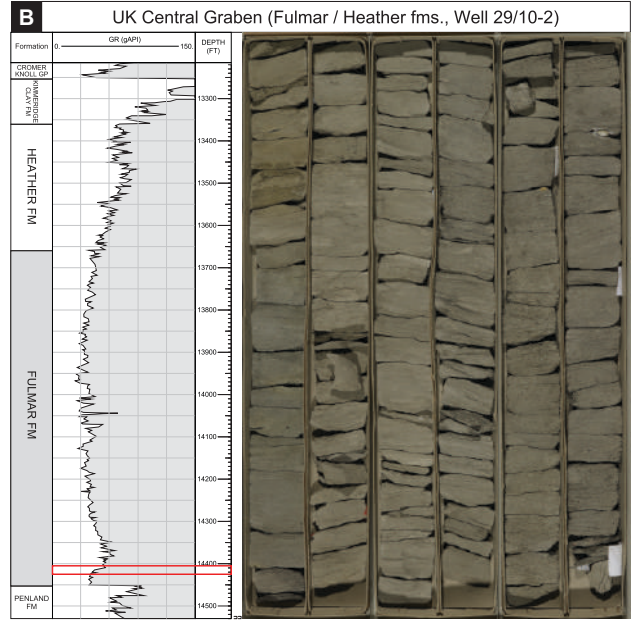
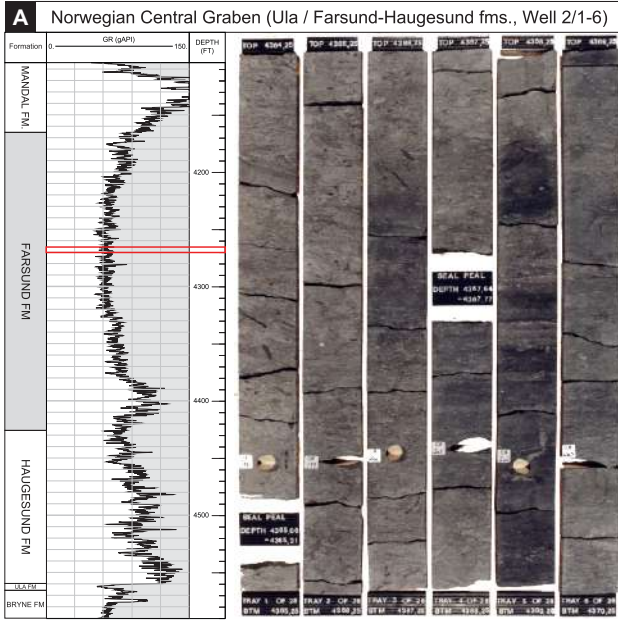


Figure 9



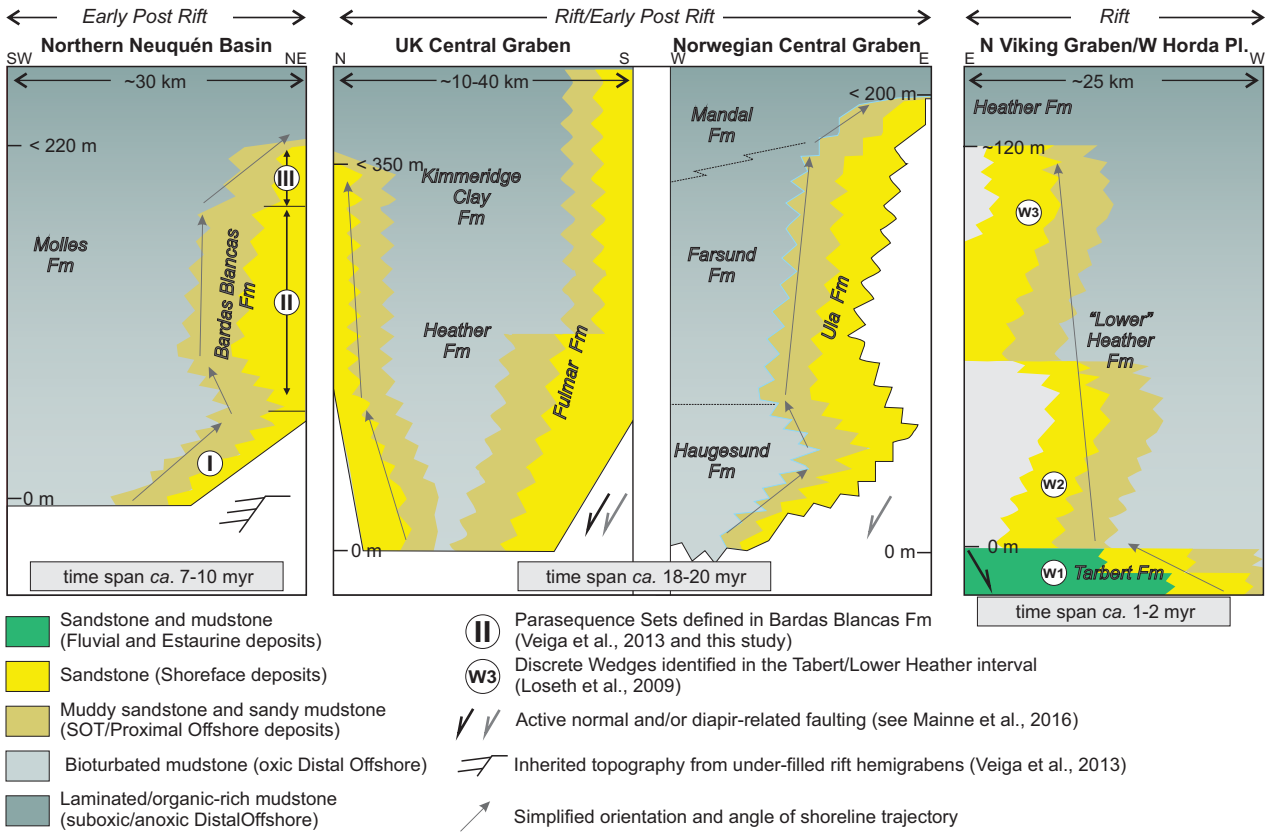


# Figure 10



cored interval shown

# Figure 11



Code	Texture	Structures	Thickness	Fossil content	Bioturbation	Trace fossils	Other	Presence	Interpretation	Environment
FA1	Normally- to inversely-graded pebbly to medium-grained sandstones.	Plane bed, planar or trough cross-stratification (sets <0.3 m thick), oriented to W-SW.	0.3–1.5 m thick beds.	Sand-size bioclasts common, high degree of fragmentation. Mostly from bivalves, but ammonite and belemnite fragments also present.	Absent to moderate (BI 0-3).	<i>Skolithos</i> suite: <i>Palaeophycus</i> , <i>Ophiomorpha</i> , <i>Arenicolites</i> .	Thin (up to 40 cm-thick) extraformational conglomerate layers with quartz and volcanic lithic pebbles (up to 5 cm-long) with mudstone rip-up clasts, and chaotic to organized fabric. Rare detrital glauconitic grains. Tree trunks, micaceous and organic debris preserved in bedding planes.	Only observed at the base of Bardas Blancas Fm.	High-energy nearshore setting, influenced by terrestrial input of river-related hyperpycnal flows, and partly reworked by subordinate coastal processes.	Delta front
FA2	Amalgamated fine- to medium-grained sandstones	Structureless or trough cross-stratification (sets <0.5 m thick).	0.5-1.8 m thick beds.	Occasional lenses of shells with oriented bioclasts at bed bases.	Absent to low (BI 0-2).	Where observed, <i>Skolithos</i> suite: <i>Ophiomorpha</i> .	Very well-sorted, “clean” sandstones. Locally preserved coarser grained, bioclast-rich accumulations at the top (transgressive lags).	Uncommon, only observed towards upper part of some parasequences.	High-energy nearshore setting, intensely reworked by dominant longshore currents.	Upper Shoreface
FA3	Amalgamated to tabular very fine- to fine-grained sandstones.	HCS with subordinate SCS and plane bed. Symmetrical ripple tops uncommon.	0.15–0.80 m thick beds. Few m-thick bedsets.	Lenses of shells with common bioclasts oriented parallel to bed bases.	Low-moderate to high (BI 2-5).	<i>Skolithos</i> suite: <i>Arenicolites</i> , <i>Skolithos</i> , <i>Palaeophycus</i> , <i>Ophiomorpha</i> ,	Parting lineation, micaceous and organic (plant) debris common. Occasional nodular carbonate horizons, associated with large bioclast accumulations.	Common in studied sections, mainly towards upper part of parasequences.	Moderate to high energy in marine environment, above FWWB. Common deposits of purely oscillatory and/or combined flows during storms. Amalgamation suggests erosion of fair-weather sediments.	Lower shoreface
FA4	Tabular very fine-grained sandstones and muddy sandstones, with subordinate sandy mudstones.	Typically massive due to very intense bioturbation. Occasional HCS or faint ripple cross-lamination.	Tabular beds from 0.10-0.40 m thick. Up to 1.50 m thick. Several m-thick bedsets.	Bioclasts of infaunal and semi-infaunal bivalves common. Low to moderate degree of fragmentation, articulated specimens common, occasionally preserved in life position. Belemnite and ammonite remains less common.	Mostly high (BI 5-6), occasionally moderate (BI 4).	<i>Cruziana</i> suite: <i>Teichichnus</i> , <i>Asterosoma</i> , <i>Rosselia</i> , <i>Chondrites</i> , <i>Planolites</i> , <i>Thalassinoides</i> , <i>Rhizocorallium</i> , <i>Palaeophycus</i> , <i>Phycosiphon</i> , <i>Zoophycos</i> .	Occasional preservation of sandstone beds (0.2-1.0 m thick), traceable for 100's of m. They are fine- to very fine-grained, with HCS or less commonly massive grading upwards to planar-laminated. Shells can be concentrated at their bases. Bioturbation (lam-scrum) increases from top downwards.	Broadly distributed in studied sections.	Moderate to low energy in marine environment, below FWWB. Lower proportion (or preservation) of storm deposits than lower shoreface deposits.	Offshore transition
FA5	Sandy mudstones and silty mudstones, with subordinate mudstones and muddy sandstones.	Diffuse grain-size changes, bedding contacts are diffuse, but roughly parallel.	Tabular beds from 0.20-0.80 m thick.	Fragments of ammonites and belemnites frequent, benthic macrofossils are uncommon (mostly oysters).	Mostly high (BI 5-6), occasionally moderate (BI 4).	<i>Distal Cruziana</i> suite: <i>Chondrites</i> , <i>Phycosiphon</i> , <i>Planolites</i> , <i>Teichichnus</i> , <i>Helminthopsis</i> , <i>Thalassinoides</i> , <i>Rhizocorallium</i> , diminute <i>Skolithos</i> , <i>Zoophycos</i> .	Discrete sandstone beds less common than in FA4. They show plane bed and bioturbation decreasing from top to bottom.	Broadly distributed in studied sections.	Low-energy conditions, with cohesive substrates and persistent oxic conditions. Relatively distal depositional setting, around SWWB.	Proximal offshore
FA6	Gray mudstones and/or black shales.	Massive to crudely laminated.	From cm- to several m-thick packages.	Foraminifera common.	Absent to moderate (BI 0-3).	<i>Zoophycos</i> suite: <i>Zoophycos</i> , <i>Phycosiphon</i> , <i>Chondrites</i> , <i>Scolicia</i> (?).	Occasional diagenetic nodule-rich horizons. In lower section, thin (up to 40 cm-thick) extraformational conglomerate layers, with mudstone rip-up clasts (up to 10 cm), chaotically distributed in sandstone beds or forming organized intraformational conglomerates. In upper section, remobilized or coherent black shales, typically platy, with absence of trace fossils and scarce fragments of small, thin-shelled bivalves. Cm-thick tuffaceous layers occur.	Relatively uncommon, mainly observed near base or top of unit.	Suspension settling in very low-energy conditions and devoid of bottom currents, below SWWB. Occasional gravity-flow deposits in the lower section. Dysoxic to anoxic conditions with soupy, organic-rich substrates in the upper section (and transition to Los Molles Fm).	Distal offshore

Table 1- Facies association classification, description and interpretation of the main processes and environments of deposition. Trace fossil content is listed in relative order of abundance. FWWB: Fair-weather wave base ; SWWB: Storm-weather wave base.

Table 2.

Units	Age; Duration; Thickness	Dominant facies (in lower shoreface and offshore-transition settings)	Long-term Stacking Pattern	Tectonic setting and subsidence	Sediment source	References
Emery Sandstone (Mancos Shale Fm., Utah, USA)	Upper Cretaceous; 1.8 Myr; < 250 m	Intensely bioturbated fine to medium grained sandstones; interbedded siltstones	Aggradational	High subsidence rates in foreland basin setting	Small rivers, little evidence of deltaic influence, low sedimentation rates compared to underlying and overlying units.	Edwards et al. (2005)
Ula and Farsund formations (Norwegian Central Graben)	Upper Jurassic; ca. 18.5 Myr; < 200 m	Intensely bioturbated very fine to fine grained sandstones (Ula Fm); intensely bioturbated muddy sandstones, sandy mudstones, silty mudstones, and shales (Farsund Formation)	Aggradational, retrogradational	Series of extensional fault-bounded basins and sub-basins, relative high mechanical subsidence	Not available	Baniak et al. (2014; 2015).
Fulmar Fm. and equivalent Header Fm. (UK Central Graben)	Middle- Upper Jurassic; ca. 21.1 Myr; < 360 m (typically 60-110 m)	Moderate to Intensely bioturbated fine to medium grained sandstones, uncommon HCS-sandstone beds; intensely bioturbated muddy heterolithics	Aggradational	Mechanical subsidence and/or diapir- related faulting, complex topography linked to sub-basins and intrabasinal highs.	Poorly developed river systems; lack large deltaic systems;	Gowland (1996); Howell et al. (1996)
Tarbert - Lower Heather formations (northern North Sea)	Middle Jurassic; < 4.2 Myr; < 200 m	Bioturbated and HCS-dominated very fine to medium grained sandstone; bioturbated siltstones	Retrogradational	Series of extensional fault-bounded basins and sub-basins, relative high mechanical subsidence	Not available	Løseth et al. (2009)
Bridport Sand Fm. (Wessex Basin, UK)	Early Jurassic; ~ 7 Ma; < 200 m	Silty, very fine to fine grained sandstones	Progradational, aggradational	Extensional fault-bonded depocentres; high rates of mechanical subsidence	Lack of river-mouth processes; along-shore transport significant; high net siliciclastic sediment input	Morris et al., 2006
<b>Bardas Blancas Fm. (Nequén Basin, Argentina)</b>	Lower to Middle Jurassic; ~ 7-10; < 220 m	Intensely bioturbated sandy mudstones, muddy sandstones, very fine to fine grained sandstones	Aggradational, Retrogradational	Underfilled rift depocentres; inherited topography	Lack of river-mouth processes; along-shore transport significant	Veiga et al., 2013; <b>this study</b>